Discovery and clinical translation of novel glaucoma biomarkers

Gala Beykin[a], **Anthony M. Norcia**[b], **Vivek J. Srinivasan**[c,d,***], **Alfredo Dubra**[a,**], **Jeffrey L. Goldberg**[a,*]

[a]Spencer Center for Vision Research at Stanford University, 2370 Watson Ct, Palo Alto, CA, 94303, USA

[b]Department of Psychology, Stanford University, 290 Jane Stanford Way, Stanford, CA, 94305, USA

[c]Department of Biomedical Engineering, University of California, Davis, One Shields Ave, Davis, CA, 95616, USA

[d]Department of Ophthalmology and Vision Science, University of California Davis School of Medicine, 4610 X St, Sacramento, CA, 96817, USA

Abstract

Glaucoma and other optic neuropathies are characterized by progressive dysfunction and loss of retinal ganglion cells and their axons. Given the high prevalence of glaucoma-related blindness and the availability of treatment options, improving the diagnosis and precise monitoring of progression in these conditions is paramount. Here we review recent progress in the development of novel biomarkers for glaucoma in the context of disease pathophysiology and we propose future steps for the field, including integration of exploratory biomarker outcomes into prospective therapeutic trials. We anticipate that, when validated, some of the novel glaucoma biomarkers discussed here will prove useful for clinical diagnosis and prediction of progression, as well as monitoring of clinical responses to standard and investigational therapies.

Keywords

Glaucoma; Nerve fiber layer; Axonal degeneration; Retinal ganglion cell; Retinal imaging

1. Introduction

Glaucoma, the leading cause of irreversible blindness worldwide, is commonly viewed as a neurodegenerative disease with multifactorial origin, and is characterized by progressive loss of retinal ganglion cells (RGCs). Although there are different subtypes of glaucomatous optic neuropathy, all result in irreversible visual field loss and blindness. Currently, glaucoma screening and diagnosis, as well as severity classification, progression monitoring, and response to medical treatment or surgical intervention are based on an experts'

impression using the combination of clinical exam, intraocular pressure (IOP) measurements, visual fields and structural imaging parameters. In the earliest stages of glaucoma when visual symptoms are absent or mild, diagnosis might be missed or delayed. Screening techniques based on IOP have poor sensitivity, as for example, over 50% of primary open angle glaucoma (POAG) patients have an IOP that is within normal range (Sommer et al., 1991b). Thus, merely using IOP greater than some number (e.g. 21 mm Hg) is not an adequate tool for glaucoma screening. Similarly, optic disc cupping does not demonstrate sufficient sensitivity and specificity as a predictor of glaucoma (Harper and Reeves, 1999). Detecting progression with visual field testing or optic disc imaging as discussed further below are limited by their retrospective nature and high variability. Currently, clinical, functional and structural tests suffer from both their need for baseline examination, as well as the significant lag time required to establish disease progression and response to treatment. In addition, RGCs may enter a dysfunctional state prior to cell death, which with therapy may be reversible (see Fig. 1) (Fry et al., 2018). There is thus a significant unmet need for glaucoma-related biomarkers to improve clinical testing, both for early diagnosis and also for detection of disease progression. We anticipate that this will allow for timely intervention in the clinic to assist in predicting prognosis and monitoring treatment response, as well as for more rapid early phase clinical trial design, for example for testing candidate neuroprotective therapies.

The United States National Institutes of Health Biomarkers Definitions Working Group defined a biomarker as "a characteristic that is objectively measured and evaluated as an indicator of normal biological processes, pathogenic processes, or pharmacologic responses to a therapeutic intervention" (Biomarkers Definitions Working, Group, 2001). Examples of biomarkers range from pulse rate and blood pressure through basic chemistries to more complex laboratory or imaging tests. The identification of biomarkers for clinical utility requires statistical validation of reproducibility, specificity, and sensitivity (Strimbu and Tavel, 2010; Drucker and Krapfenbauer, 2013), and the determination of relevance. Relevance refers to a biomarker's ability to provide information that will eventually affect clinical decisions and endpoints. For glaucoma, the currently most used clinical biomarker outside of IOP screening, i.e., visual field testing, has been extensively reviewed elsewhere (Wu and Medeiros, 2018; Zhang et al., 2019b) and thus important advances in instrumentation, testing protocols and analyses will not be covered here.

What else could such biomarkers target for measurement? Certainly molecular biomarkers are enticing as a target. Recent experimental studies have advanced our understanding of the pathophysiology of glaucomatous neurodegeneration. However, molecular and cellular mechanisms initiating and propagating the neuronal injury of RGCs, the cross-talk between various degenerative pathways, and the contribution of each pathway to structural and functional loss, remain largely unknown. Imaging biomarkers for glaucoma may exploit structural or functional image contrast that could be used to evaluate disease at a single time point or detect changes. Imaging of the optic nerve include classical stereo disc photography, red-free observation of nerve fiber layer defects (Hoyt et al., 1973), optical coherence tomography (OCT) visualization of the nerve fiber layers. Additional imaging modalities are available, such as OCT angiography (OCTA) which enables visualization of perfused retinal vasculature (Miguel et al., 2019), adaptive optics scanning light ophthalmoscopy (AOSLO)

for visualization of cellular and subcellular details, and even high-resolution magnetic resonance imaging (MRI) to examine features of the retro-bulbar optic nerve and visual pathway (Lagrèze et al., 2009). Electrophysiological testing may allow objective evaluation of function of different locations, pathways and cell types of the visual system.

Where to search for such molecular, electrophysiological and imaging biomarkers? The primary neurodegeneration of glaucoma takes place in the optic nerve and inner retina, but to biopsy these tissues would not be clinically plausible. Surveying the vitreous fluid and serum is less invasive, and the aqueous humor and the tear film have also been proposed as even more accessible, albeit slightly more distant sites for molecular biomarkers. Optical imaging with a focus on RGCs' dendrites in the inner plexiform layer, cell bodies in the ganglion cell layer (GCL), and axons in the nerve fiber layer and optic nerve head, on the other hand, is particularly attractive due to its non-invasiveness. Measuring and recording electrical signals produced during neural transduction along the visual system may reveal sensitive information about physiological versus pathological neuronal function, potentially important at early stages. Here we review progress towards uncovering molecular, electrophysiological and imaging biomarkers, organized by associated pathophysiologic targets of RGC dendrite degeneration, cell body death, axon loss, and metabolic deficit, followed by a survey of molecular biomarkers that may be germane to these. We defer reviewing imaging of the anterior segment of the eye to assess the iris, the anterior chamber and the trabecular meshwork in glaucoma patients (Zotter et al., 2012). Finally, we discuss the implications of these data and next steps and argue that the discovery and validation of structural or functional biomarkers may indeed lead to deeper understanding of the disease itself.

2. RGC axon degeneration

Although the exact cause of RGC degeneration is still unknown (Marcic et al., 2003; Kuehn et al., 2005; Davis et al., 2016), observations with fundoscopy indicate that nerve fiber layer defects might be, currently, the earliest clinical signs of glaucomatous optic nerve atrophy (Hoyt et al., 1973). This is supported by animal studies showing axon dysfunction and degeneration preceding neuronal loss (Buckingham et al., 2008; Howell et al., 2013). Certainly, localized defects and in some cases generalized reduction of RNFL thickness takes place not only in patients with glaucoma but also in those with ocular hypertension (OHTN) and other neurodegenerative diseases (Airaksinen et al., 1984; Khanifar et al., 2010). RNFL thickness monitoring has been shown to be more sensitive than color disc evaluation in the detection of progressive damage at early stages of glaucoma (Quigley et al., 1992). In longitudinal studies, the vast majority of glaucoma patients had demonstrable RNFL abnormalities at least 3–6 years before the onset of field loss (Sommer et al., 1977, 1984, 1991a) with a strong correspondence between anatomical location of RNFL abnormalities and visual field defects (Quigley et al., 1980b). These data indicates the need to examine the RGC axon as a locus of pathology in glaucoma (Buckingham et al., 2008).

2.1. Optical coherence tomography

Although red-free fundus photography can be used for the identification of localized nerve fiber layer defects in glaucomatous eyes (Jung et al., 2018), it remains qualitative and subjectively interpreted. How to better image and quantify nerve fiber layer defects? The earliest and still most widely-used quantitative metric of axon atrophy or loss in glaucoma is RNFL thickness (Schuman et al., 1995a), segmented in a circumpapillary OCT image centered on the optic nerve head. RNFL thinning is associated with loss of RGC axons in glaucoma, which occurs on top of an age-related loss (Schuman et al., 1995b). Although normative databases are available against which to compare patients and render diagnoses, circumpapillary RNFL thickness may be most useful to track longitudinal changes over time (Wollstein et al., 2005) because progressive axon degeneration consistent with glaucoma can often be detected before visual field dysfunction is detectable (Wollstein et al., 2012). Additionally, RNFL thickness is most informative about progression in mild to moderate glaucoma, as in more advanced staged RNFL thickness reaches a floor beyond which it is not possible to further monitor progression of severe glaucoma (Mwanza et al., 2015). The application of RNFL and related techniques that assess axons at the neuroretinal rim (Chauhan et al., 2013) to glaucoma diagnosis and progression has been studied extensively over the prior decade. Although purely structural, these measures owe their success to their reproducibility and objectivity, benefitting from advances in technology and algorithms, which have been reviewed elsewhere (Hood, 2017).

One major limitation of RNFL thickness as a biomarker for RGC axon loss is that the RNFL also includes astrocytes, Muller cell end-feet, and vascular structures, all of which contribute to RNFL thickness independent of RGC axon degeneration. Thus, alternatives have been explored. The RNFL topography derived from OCT imaging may be an alternative biomarker to RNFL thickness (Lin et al., 2017). For a given rate of RNFL thinning, the reduction in the RNFL reflectance intensity compared to that of the retinal pigment epithelium was associated with more rapid functional deterioration (Gardiner et al., 2016) and may indicate disease in the pre-perimetric stage (Liu et al., 2014). Reflectance intensity may decrease prior to losses in thickness, suggesting that a decrease in RNFL reflectance near the ONH may serve as an early sign of glaucomatous damage (Huang et al., 2011; Zhang et al., 2011; van der Schoot et al., 2012). This technique displayed good agreement with and was strongly related to RNFL thickness measures, providing a useful approach for identifying regions of potential RNFL abnormality for targeted perimetry (Ashimatey et al., 2018a). Retinal contour variability, a circumpapillary spatial frequency metric tailored to separate glaucoma from normal subjects, revealed small-scale focal damage, thus providing different diagnostic information but perhaps synergistic with broader thickness measures (Tan et al., 2016). In addition, a novel technique for quantifying RNFL bundle abnormality in the temporal raphe identified reflectance abnormality when perimetric abnormality was present, mild or even absent. The findings support the potential of raphe imaging in detecting early glaucomatous damage (Ashimatey et al., 2018b).

The cylindrical structure of RNFL axons contributes to birefringence. While scanning laser polarimetry (Cense et al., 2004; Gotzinger et al., 2008; Yamanari et al., 2008; Zotter et al., 2013; de Boer et al., 2017) measures the total birefringence, or more strictly, retardance, of

the RNFL, polarization sensitive (PS) OCT can assess birefringence and thickness independently. Cylindrical structures contributing to optical property of birefringence include axonal membranes, microtubules, neurofilaments and mitochondria. The decrease of RNFL birefringence in glaucoma may indicate a loss of microtubules (Huang and Knighton, 2005), making PSOCT a potentially useful technique for the early detection (Cense et al., 2002). While an assessment of subcellular RGC axon health in otherwise intact axons is appealing, PSOCT must solve issues of instrumentation complexity and calibration to realize this promise (Liu et al., 2018; Swanson et al., 2019).

2.2. Adaptive optics-enhanced optical coherence tomography

Can higher transverse resolution get us closer to measuring the disease process in RGC axons? Adaptive optics (AO) ophthalmoscopy has allowed for *in vivo* visualization of retinal structures beyond the lateral resolution of conventional OCT and fundus photography, down to individual axon fiber fascicles (bundles) (Zawadzki et al., 2008; Cense et al., 2009; Torti et al., 2009; Kocaoglu et al., 2011, 2014; Takayama et al., 2012; Chen et al., 2015a; Hood et al., 2015a). Progressive axon fascicle loss in glaucoma was shown on reflectance AO scanning light ophthalmoscopy to be associated with subsequent development of deep defects on visual fields at a time that these changes are still below the spatial resolution of even the perifoveal 10-2 Humphrey visual field (HVF).

2.3. Reflectance confocal adaptive optics scanning ophthalmoscopy

As with conventional OCT, the interpretation of *en face* AO-enhanced OCT images is challenging due to the presence of high contrast grains or speckles due to interference of light within microscopic features. AO-enhanced reflectance confocal scanning light ophthalmoscopy (AOSLO) is less affected by this problem, albeit at the cost of an order of magnitude axial resolution. This complementary approach has been used to study the inner surface of the RNFL in normal (see Fig. 2) and glaucomatous subjects (Chen et al., 2015a; Hood et al., 2015a, 2015b, 2017) revealing micron-sized hyper-reflective spots along the axon bundles. These spots, seen as a continuum in conventional OCT due to diffraction blur, are the source of the characteristic RNFL reflectivity. Interestingly, the reflectivity of individual spots, which are of dimensions that might be consistent with axonal varicosities, change dramatically over the span of a few seconds to minutes (see Fig. 2), potentially being indicative of axonal transport. The reflectivity of these RNFL spots averaged within axons bundles at single time points has been qualitatively studied by and compared with conventional OCT imaging in a small glaucoma cohort (Chen et al., 2015a). Reflectance AOSLO revealed areas of reduced reflectivity and contrast near and within arcuate defects, both before and after RNFL thinning, leading to the hypothesis that reduction of RNFL intensity along arcuate defects (whether in conventional OCT or AOSLO) might reveal glaucomatous damage before RNFL thinning. This lower reflectivity could be clinically relevant as it might be easily observable in conventional OCT instruments, if the images were displayed in a linear intensity scale, rather than the usual logarithmic scale. Therefore, and despite the current data suggesting that RNFL reduction of reflectivity and thinning might not always occur in the same order, a combination of AOSLO and conventional OCT might be useful in clinical trials with modest number of subjects, to detect minute transverse and axial RFNL changes.

Reflectance AOSLO has also showed that progressive axon fascicle loss in glaucoma is associated with subsequent development of deep defects on visual fields at a time that these changes are still below the spatial resolution of even the perifoveal 10-2 HVF. Subtle global thinning of axon fascicles across the retina, however, cannot be measured with this imaging modality which best measures focal changes, and thus, diffuse thinning may be better followed with OCT (see Fig. 3) (Hood et al., 2017).

Although AO imaging is a powerful retinal imaging toll providing high transverse resolution enabling noninvasive imaging of cellular and subcellular structures, the technology still poses some limitations withholding this modality from breaking into wide and routine clinical implementation yet. Among its limitation is the small field of view that can be imaged while providing high resolution, even when using advances techniques (Laslandes et al., 2017). In addition, optical media opacities can interfere with optimal imaging due to decrease in image quality (Pilcher and Zawadzki, 2017).

RNFL speckle pattern observed in conventional OCT, due to the temporal coherence of the light source, arises from light scattered by axonal cargo and/or structure, and might be related to the intensity changes observed in reflectance AOSLO mentioned above. The dynamics of this speckle pattern are likely related to axonal transport (Brown, 2003; Wang et al., 2003; Huang et al., 2013); a measure of which, though challenging, could be an early biomarker of stress.

2.4. Imaging the visual pathway into the brain

Axon degeneration of RGCs can also be measured in the optic nerve and potentially the optic tract using MRI. MRI-based protocols such as diffusion tensor imaging can detect intracranial myelination abnormalities by metrics including fractional anisotropy related to diffusion of water. These have been investigated in glaucoma and show variable correlations with RNFL thickness measured by OCT (Lagrèze et al., 2009; Engelhorn et al., 2012; Zhou et al., 2017). A different diffusion tensor imaging study with whole-brain voxel-based analysis (El-Rafei et al., 2011) displayed altered parameters in the optic chiasm and optic radiations of glaucoma patients correlating with disease stage, and thus could serve as potential noninvasive markers of disease severity (Dai et al., 2013a). Thus there are somewhat conflicting data thus far for glaucoma, and these could be further explored, particularly in comparison to other optic neuropathies in search of biomarker specificity.

MRI can also reveal degeneration downstream of RGC axons in the visual pathways to the brain. Downstream of RGC axons, degeneration of the lateral geniculate nucleus (LGN), geniculo-cortical projections, and cortical areas themselves have been explored in glaucoma patients. Evidence of LGN atrophy has been detected in some glaucoma patients (Gupta et al., 2009). Magnetization transfer imaging is a sensitive MRI technique that suggests geniculocalcarine demyelination and striate area degeneration in primary glaucoma, and in another study an increase in the number of white matter hyperintensities suggests that cerebrovascular disease may also play a role in the pathogenesis of POAG (Kitsos et al., 2009; Zhang et al., 2016). Furthermore, a study combining OCT and multi-modal MRI found that inner retinal layer thinning, optic nerve cupping and reduced visual cortex activity occurred before patients showed visual field impairment. Furthermore, choline metabolism

within the visual cortex was perturbed along with increasing disease severity in the eye, optic radiation and visual field (Murphy et al., 2016). Similar investigations using MRI and optokinetic assessments are finding structural and physiological changes in the eye and anterior and posterior visual pathways in mouse model of chronic glaucoma (Yang et al., 2018).

Exploring these neurodegenerative effects downstream in the brain has raised the question of whether such central changes are in any way primary or causative in glaucoma pathophysiology. Earlier detection may be achieved if such central changes precede retinal or (ONH) pathologies, or simply if brain measures happen to be more sensitive than retinal measures. Based on the weight of the data supporting ONH and retinal pathophysiologies, we suggest that changes in the brain are mainly secondary effects of anterograde axonal and even trans-synaptic degeneration. Nevertheless, the sensitivity of different structural or, discussed below, functional assays of the full visual pathway may shed light onto eye-brain interactions across disease severity, metabolic changes occurring in the brain's visual system in glaucoma, and the utility of such measures to detect or stage the disease (see Fig. 4) (Kasi et al., 2019). Of course, although the eye is the most accessible organ for direct, high-resolution imaging, we believe that MRI data will continue to contribute to deepening our understanding in experimental models, even if it will not be frequently used for routine clinical imaging of glaucoma patients.

3. RGC dendritic changes

The inner plexiform layer (IPL), comprising dense connections between bipolar cell axons, amacrine cells, and ganglion cell dendrites, is another prime site for investigating both glaucoma pathophysiology and biomarker development (Agostinone and Di Polo, 2015). A number of functional and molecular pathways implicated in glaucoma have been localized to the IPL synapses (Stevens et al., 2007; Howell et al., 2011; Agostinone et al., 2018), and RGC dendrite degeneration or remodeling is observed early in disease in animal models, and particularly may be detected earliest in "OFF" RGCs, the dendrites of which are in the outermost lamina of the IPL (Della Santina et al., 2013; El-Danaf and Huberman, 2015; Ou et al., 2016; Puyang et al., 2017) (see Fig. 5). However, while somatic (GCL) and axonal (RNFL) loss in glaucoma have been extensively studied with OCT, comparatively few studies report IPL changes in human glaucoma. One reason for this is the inherently low reflectivity contrast between the GCL and IPL. In commercial OCT instruments, the IPL has historically been grouped with the GCL in a macular ganglion cell–inner plexiform layer (mGCIPL) thickness measurement. In studies where the IPL has been successfully segmented (Kim et al., 2016, 2017a; Chien et al., 2017), it is not clear if total IPL thickness decreases in concert with GCL and NFL thickness in glaucoma. A recent study (Moghimi et al., 2019) suggested that IPL thickness is not preferentially decreased relative to GCL thickness in glaucoma. This is not necessarily inconsistent with animal studies that point to early dendritic rearrangements that may not cause IPL thinning. Interestingly, only one *in vivo* imaging study, to our knowledge, has explicitly attempted to examine the sublaminar structure of the IPL, qualitatively comparing its reflectivity pattern to sublamination observed histologically (Tanna et al., 2010). Other studies have occasionally visualized apparent internal structure within the IPL, but did not explicitly comment on its appearance

(Szkulmowski et al., 2012). Ultimately, the imaging data on the internal IPL structure in the literature remain sparse and anecdotal.

Data from a small cohort of glaucoma and control subjects using a near-infrared commercial OCT suggests that irrespective of the image segmentation method, the IPL reflectivity maps show poor repeatability (see Fig. 6). IPL thickness, however, shows greater promise as a glaucoma biomarker. In fact, our initial investigation of IPL structure using commercial instruments underscored the need for better axial resolution to resolve IPL sub-laminae. As axial resolution of OCT is inversely proportional to the center wavelength of the imaging light, we explored the use of visible light OCT (Shu et al., 2017) with a custom instrument. This visible light OCT imaging enabled the visualization of internal structure of the IPL in both mice (Kho and Srinivasan, 2019) and humans (Zhang et al., 2019a) (see Fig. 7). The 3 hyper-reflective bands and 2 hypo-reflective bands observed with visible light OCT correspond well with the standard anatomical division of the IPL into 5 layers (Koontz and Hendrickson, 1987). Laminar differences in synapse density or in neurite orientation, size, or density may generate this reflectivity contrast. If the anatomical strata coincide with the reflective bands as we tentatively suggest, the ON- and OFF-sublaminae can be quantified in human subjects. Thus, our preliminary data suggest IPL sublaminar thickness, reflectivity, and/or contrast may be promising biomarkers for early dendritic changes and thereby for glaucoma diagnosis or progression. Cohort and longitudinal studies as well as ongoing improvement in imaging hardware, scanning protocols and image processing are our next steps towards these goals.

4. RGC cell bodies and apoptosis

As part of the disease process in glaucoma and other optic neuropathies, RGCs undergo apoptosis, or programmed cell death. RGCs and their much broader surrogate the GCL are already being investigated heavily using OCT as discussed above. Changes in macular parameters like mGCIPL thickness in eyes with early or advanced glaucoma might be detected more sensitively than RNFL (Wong et al., 2012). The value of RNFL and mGCIPL measurements may vary at different stages of disease, with macular measurements being helpful in assessing damage in the earliest and latest stages, especially when beyond the floor observed in circumpapillary measurements (Sung et al., 2012; Bowd et al., 2017; Kim et al., 2017b).

Newer high-speed swept-source OCT (ssOCT) technologies (Lim et al., 2006; Srinivasan et al., 2007) allow for faster acquisition with reduced motion artifact at the cost of slightly lower axial resolution due to the use of longer wavelengths. A novel method for estimating the number of RGCs indirectly from ssOCT-derived RGC layer thickness measurements was recently demonstrated (Raza and Hood, 2015). Nevertheless, it is important to remember that just as the thickness of the RNFL is influenced by glial and other cells beyond RGC axons, similarly the thickness of the GCL is influenced by many other cell types beyond RGCs, including astrocytes, Muller glia, and displaced amacrine cells. Thus, motivation to move past OCT imaging of layer thickness remains high.

4.1. Dye-based detection of apoptosing retinal cells

Utilization of dyes to measure RGC apoptosis is an exciting approach with supportive early data. Detection of apoptosing retinal cells (DARC) takes advantage of translocation of plasma membranes' phosphotidylserine from internal to external leaflet at early stages of apoptosis. Externalized phosphotidylserine can be labeled with a fluorophore-tagged high-affinity binding protein annexin V, thereby marking RGCs undergoing apoptosis. DARC has been intensively studied in animal models investigating both neurodegeneration pathophysiology and possible neuroprotective treatments (Yap et al., 2018a). In humans, a successful phase I clinical trial (ClinicalTrials.gov Identifier: NCT02394613) was recently completed and demonstrated that DARC provides minimally invasive *in vivo* real-time signals that correlate with disease severity (see Fig. 8) (Cordeiro et al., 2017). Hopefully, next steps will include longitudinal imaging with this technique, and at some point, dissection of cell type specificity and distinction between dysfunctional and truly apoptotic cells.

4.2. Label-free RGC imaging

Direct counting of RGCs and/or measuring cellular features that presage cell dysfunction or death would likely result in a diagnosis and progression monitoring paradigm change and, therefore, the recent progress towards non-invasive and label free imaging of RGCs in humans has generated a lot of excitement. Non-confocal AOSLO reflectance imaging (Rossi et al., 2017) has shown 2-dimensional views of the RGC mosaic with very modest contrast (Scoles et al., 2013), and more recently, AO-OCT has enabled diffraction-limited resolution images of the optic nerve head and retina in three-dimensions, increasing resolution down to a theoretical $3~\mu m^3$, enabling visualization of the micro-structure of the lamina cribrosa (LC) (see Fig. 9) (Dong et al., 2017). This has enabled imaging of RGC somas with much greater contrast and in 3-dimensions, even in regions when the GCL is multiple cells deep (Liu et al., 2017). This AO-OCT imaging exploits the motion of cellular organelles over the span of minutes as both a novel source of image contrast and a means to average out the image speckle that typically affects OCT images. In its current form, this approach requires the capture of numerous image volumes (in the order of 100) over a 5- to 10-min period per retinal location (1–3° per field of view), which limits this imaging to a very small retinal area per imaging session. Key next steps could include differentiating RGCs from amacrine cells or identifying RGC subtypes via optical signatures, with the caveat that RGC soma loss occurs relatively late in the disease process, well after RGCs show initial signs of stress and dysfunction (Buckingham et al., 2008; Chang and Goldberg, 2012).

4.3. INL changes in glaucoma and other diseases

Other non-specific inner retinal findings have been documented with AOSLO multiple-scattering imaging, including inner nuclear layer (INL) micro cystoid spaces (see Fig. 10, Fig. 11 and Fig. 12) found to be closely associated with RNFL and GCL thinning and correlated with worse mean deviation (MD) slope (Scoles et al., 2014; Hasegawa et al., 2015; Wells-Gray et al., 2018). These INL micro cystoid spaces, sometimes visible in conventional OCT imaging (Hasegawa et al., 2015) have been reported in various conditions that affect the optic disc, including multiple sclerosis, neuromyelitis optica and hereditary

optic neuropathy (Wolff et al., 2013, 2014; Carbonelli et al., 2015; Chen et al., 2015b). The non-confocal split-detection AOSLO images below (Razeen et al., 2018) reveal some important characteristics of these micro cystoid spaces. First, their dimension, spacing and distribution across the macula being highly variable across eyes, with size alone ranging from a few microns to tens of microns (see Figs. 10 & 11). Importantly, these micro cystoid spaces appear in areas of reduced, but not complete, vision loss, suggesting their potential as a biomarker of progression. In fact, their sensitivity as a biomarker is potentially superior to RNFL thickness or visual fields, as their development and resolution can be clearly observed in as little as four weeks.

5. Optic nerve head morphology and deformation

The greater than one million ganglion cell axons pass to the brain from the eye via the ONH, traversing the LC, a porous connective tissue structure comprised of collagenous beams and a population of astrocytes. From an imaging biomarker standpoint, the ONH provides the opportunity to assess all RGC axons at a single location, with sectoral resolution. Glaucomatous ONHs are classically characterized on examination or fundus photography by generalized or focal enlargement of the cup (Armaly, 1970), disc hemorrhages, thinning of neuroretinal rim, inter-eye cup asymmetry (Ong et al., 1999; Hawker et al., 2005; Ramakrishan et al., 2013) and/or beta zone (parapapillary region defined by the existence of Bruch's membrane and absence of retinal pigment epithelium) atrophy (Bourne, 2006; Dai et al., 2013b). These signs reflect loss of nerve fibers and serve as markers of glaucoma risk. Since Bruch's membrane is invisible and the angle of axons exiting the eye may vary relative to the Bruch's membrane plane, which is not considered in fundus images (Chauhan and Burgoyne, 2013), OCT has been used for more quantitative evaluation of these disc parameters (Mokhtari et al., 2019). Although RNFL thickness is currently the most commonly clinically used OCT metric, ONH parameters such as rim area (Na et al., 2013; Lavinsky et al., 2018), minimum rim width (Chauhan et al., 2013; Gardiner et al., 2014), and other elements of disc evaluation (O'Connor et al., 1993) can reveal structural progression in some cases as or more sensitively than changes in RNFL thickness.

What biology at the ONH could shed further light on glaucoma pathophysiology or biomarker development? The LC may play a role in transducing the intraocular-extraocular pressure gradient onto axons, and is thought to be a primary site of damage and/or progression in glaucomatous optic neuropathy. Early experimental studies suggested mechanical compression and blockage of axonal transport as a primary mechanism of ONH damage in glaucoma (Quigley et al., 1980a). The notion of changes in ONH connective tissues as prognostic markers in glaucoma was initially based on *ex vivo* serial sections in experimental primate models (Burgoyne et al., 2004). Recent improvements in OCT scan speed have enabled visualization of the porous structure of the LC *in vivo* (Potsaid et al., 2008; Srinivasan et al., 2008). OCT studies have revealed glaucomatous micro-architecture changes in the LC, including reduction in pore size and increased pore size variability (Wang et al., 2013)and LC thickness (Omodaka et al., 2015). In other studies, the rate of posterior LC displacement correlated with the progression of visual field defects (Wu et al., 2017; Kim et al., 2018). The addition of AO to ssOCT enabled high resolution, deep penetration, and further characterization of the LC (Zawadzki et al., 2009; Nadler et al., 2014; Jian et al.,

2016), including in animal models of experimental glaucoma (Vilupuru et al., 2007; Ivers et al., 2015). Thus deep ONH imaging can assess connective tissue (and supporting microvasculature, see below) directly at a putative site of axonal injury, and may provide meaningful IOP-independent risk stratification of subjects. Still, numerous challenges including blood vessel shadowing and light scattering in eyes with thick prelaminar tissues must be addressed through improved OCT or scanning light ophthalmoscopy systems (Sigal et al., 2014), and structural or biomechanical measurements at the lamina would be even more powerful with a direct biomarker of cellular stress.

Along these lines, a series of recent studies has lent support to the notion that low cerebrospinal fluid pressure, or intracranial pressure (ICP), is a risk factor for glaucoma (Berdahl et al., 2008; Berdahl and Allingham, 2010). This is logical since anteriorly directed ICP and posteriorly directed IOP create a translaminar pressure gradient which is thought to cause pathology of the LC and alter axonal transport. However, while low ICP may signify biomechanical risk that IOP measurement cannot capture, and thus has great potential utility as a glaucoma biomarker, we currently lack a robust and direct non-invasive measure of ICP that can be routinely used as a screening tool (Siaudvytyte et al., 2015), though some techniques have shown potential (Price et al., 2019). At best, such a measure, in concert with IOP, could predict much of the variability in glaucomatous damage that is not explained by IOP alone.

6.   Blood flow, oxygen, and metabolic dysregulation

In the normal inner retina, blood flow delivers oxygen and nutrients to meet the metabolic demands of neuronal activity (Ventura and Porciatti, 2006) and active transport (Bach et al., 2006). Observations of changes in ocular blood flow and vessel parameters in glaucoma patients have supported the long-standing model for vascular dysregulation in glaucoma pathophysiology (Flammer, 1994; Gugleta et al., 2007, 2013b). Oxygen metabolism and underlying energetic requirements are impaired in early glaucoma (Kong et al., 2009; Crish et al., 2010; Wong-Riley, 2010), possibly before structural changes occur. Molecular investigations have suggested increased expression of hypoxia-inducible factor-1α (HIF-1α) in human eyes with glaucoma at retinal locations corresponding to visual field defects (Tezel and Wax, 2004; Mozaffarieh et al., 2008). Candidate protective or regenerative therapies such as neurotrophic factors may act in part through affecting oxygen consumption and blood flow. For example, ciliary neurotrophic factor (CNTF) regulates both maximal oxygen consumption and associated spare respiratory capacity in neuronal cultures (Orgul, 2007; Hill et al., 2009), and brain-derived neurotrophic factor (BDNF) regulates cerebral blood flow (Saleh et al., 2013). Thus blood flow, vascular autoregulation, and oxygenation are promising biological targets for monitoring retinal and optic disc degeneration and therapeutic responses.

6.1.   Measuring flow

A variety of studies on oxygenation and flow in glaucoma have been performed over the past few decades, using techniques with varying degrees of depth resolution and quantification. Early techniques, such as dynamic laser speckle imaging (Sugiyama et al., 2010; Wei et al.,

2012), were relative rather than absolute, and therefore challenging to compare across eyes. Doppler ultrasound (Zakharov et al., 2009; Hwang et al., 2012; Sehi et al., 2014) can only measure flow in major vessels. Laser Doppler flowmetry (Wang et al., 2009a), although capable of providing quantitative data, lacks depth discrimination and is therefore affected by morphological changes such as tissue loss in the RNFL (Riva et al., 1972).

More advanced techniques are now being applied to image blood flow dysregulation in glaucoma. Depth-resolved Doppler OCT can quantify layer-specific blood flow in arteries and veins (Riva et al., 2010; Doblhoff-Dier et al., 2014; Leitgeb et al., 2014), with auto-correlation techniques showing promise in quantifying red blood cell velocity in retinal capillaries (Wang et al., 2009b; Jia et al., 2012b; Srinivasan et al., 2012). Quantification of blood flow has been aided by robust angle-independent methods (Wang et al., 2008; Srinivasan et al., 2010; Baumann et al., 2011). Commercial systems' OCTA algorithms for smaller capillary identification, ONH flow index (Jia et al., 2014), peripapillary flow index (L et al., 2015), and peripapillary vessel density (Liu et al., 2015) have now allowed assessment of macular and peripapillary microvasculature with better depth-resolution and more non-invasively than fluorescein angiography (Jia et al., 2012a). Other progress in using OCTA as a biomarker for glaucoma diagnosis or detection of progression has accelerated in recent years and has been reviewed elsewhere (Kashani et al., 2017; Alnawaiseh et al., 2018; Hollo, 2018). Color Doppler imaging and laser speckle flowgraphy have complemented OCTA to describe blood flow changes in glaucoma patients (Martinez and Sanchez, 2005; Zeitz et al., 2006; Mursch-Edlmayr et al., 2018), but may have limited utility next to OCTA (Kiyota et al.,2018; Takeyama et al., 2018). A new study combining line-scanning Doppler flowmetry and OCT was able to provide ultra-widefield dye--free visualization of retinal and choroidal vasculature in humans and animals (Mujat et al., 2019), with the potential to also derive precise and quantitative local flow parameters. Taken together, longitudinal studies are still needed, and based on data to date, we hypothesize that blood flow may only decrease secondary to neuronal loss and reduced demand in many cases of glaucoma, thus providing limited information about future progression. However, such glaucoma-related secondary blood flow dysregulation may serve as important biomarkers for objective severity classification of the disease, and therefore comprise an important parameter for decision upon treatment approach.

6.2.   Moving from flow to oxygen metabolism

Beyond examining blood flow to RGCs and their axons in the inner retina and optic nerve head, studying oxygen saturation and extraction could give further information about RGC energetic demands in relation to blood flow supply. Vascular oxygen saturation measurements from spectroscopic reflectance imaging with custom fundus cameras have been used to detect alterations in glaucoma (Siesky et al., 2010; Olafsdottir et al., 2011, 2014; Yap et al., 2018b), as well as in response to light flicker in glaucoma patients (Garhofer et al., 2004; Gugleta et al., 2012, 2013a; 2013b; Mroczkowska et al., 2013; Vandewalle et al., 2014). These studies have highlighted a need for quantitative measurements, which can be compared across subjects, irrespective of media opacities and fundus pigmentation. One non-invasive spectrophotometric retinal oximetry technique was used in the Leuven study, a prospective case-control study to evaluate ocular blood flow in

glaucoma, finding that the normal tension glaucoma group had similar arterial oxygen saturation but significantly higher venous oxygen saturation and arteriovenous difference when compared to POAG and healthy controls (Abegão Pinto et al., 2016). The technique for non-invasive 'two-wave' spectroscopic retinal saturation calculation, as used in the Leuven study, is based on an analysis of two simultaneous images of same fundus area taken at different wavelengths, by a system installed on a conventional fundus camera (Rilvén et al., 2017). There are some limitations of this technique. For example, results might be affected by fundus pigmentation, cataracts and vessel diameter (Rilvén et al., 2017). In addition, visible light OCT (Yi et al., 2015) is a promising technique that avoids these issues and can now measure saturation in the human retina (Chong et al., 2017). However, in the absence of simultaneous blood flow measurements, oxygen saturation is challenging to interpret, as increased venous oxygenation may reflect either increased blood flow or reduced retinal oxygen metabolism. This ambiguity is relevant for glaucoma, particularly in cases where supply and demand are uncoupled (Sehi et al., 2014) due to vascular dysregulation.

One solution to resolve these ambiguities is to measure inner retinal oxygen metabolism (MO_2). The retinal circulation provides a unique opportunity to apply Fick's principle to calculate oxygen metabolism, calculated as the product of blood flow, hematocrit and arteriovenous saturation difference. A number of approaches have been pursued for measuring flow and oxygenation in rodents (Liu et al., 2011; Song et al., 2014) . To date quantitative global retinal MO_2 has not been studied extensively enough in the human retina. Retinal oximetry may contribute to better understanding of glaucoma pathophysiology, by providing data on retinal metabolic oxygen demand, especially valuable when combined with measurements of retinal blood flow (Shughoury et al., 2020). We suggest that this should be an area of intense investigation in the future, given recent improvements in the component technologies to measure flow and oxygenation, and the potential of MO_2 to inform our understanding of glaucomatous progression.

7. Mitochondrial dysfunction

Glaucoma has not been well linked to mutations that result in mitochondrial dysfunction, however, accumulating evidence indicates that age-related mitochondrial defects play a central role in the pathogenesis of this and other neurodegenerative diseases (Kong et al., 2009; Banerjee et al., 2013). Mitochondrial dysfunction produces reactive oxygen species (ROS) which contribute to RGC apoptosis (Kortuem et al., 2000; Geiger et al., 2002; Chrysostomou et al., 2013). Additionally, RGC death may result from disturbances in axon transport (Radius and Anderson, 1981; Chang et al., 1999; Buckingham et al., 2008; Crish et al., 2010; Fu and Sretavan, 2012), and a major cargo of axon transport is mitochondria. Novel techniques for visualizing and quantifying mitochondrial dysfunction and axonal flow may thus result in the discovery of non-invasive biomarkers of glaucoma.

In vivo imaging of axonal transport of mitochondria in animals has now been extended to RGCs in glaucoma models (Takihara et al., 2015). These data showed axonal transport of mitochondria is highly dynamic *in vivo* under physiological conditions, and reduced in RGCs in early glaucoma, when RGC death was not yet dominant. In humans, AOSLO

imaging of RNFL bundles is currently being investigated for detecting axonal flow and mitochondrial function. Changes in surface reflectivity of the RNFL might be attributable to mitochondrial activity and/or axon transport. Other, non-invasive measures of cellular activity are coming through technical development to enter human testing. For example, speckle fluctuations in OCT imaging over a time scale of seconds may reflect intracellular organelle motility in both retinal pigment epithelial cells and RGCs (Liu et al., 2017), perhaps with a dependence on RGC activity (Kurokawa et al., 2018), and may also be a useful biomarker. Larger longitudinal studies will be needed to confirm these findings and quantify axonal flow in healthy controls, OHTN and glaucoma patients.

Another approach to capturing mitochondrial dysfunction and associated production of ROS takes advantage of the conversion of mitochondrial flavoproteins to their oxidized state, which produces an increase in their blue light-stimulated fluorescence (Benson et al., 1979; Shibuki et al., 2003; Kindzelskii and Petty, 2004; Reinert et al., 2004). Recently, a non-invasive method of detection of flavoprotein autofluorescence (FPF) (Field et al., 2008, 2012) showed significantly increased macular FPF in OHTN and the macular FPF/RGC+ thickness ratio in OHTN and POAG patients when compared to controls (Geyman et al., 2018). Thus, detection of mitochondrial dysfunction may be possible before structural changes are evident on current clinical imaging modalities, and such early diagnosis of dysfunction may allow study of timely intervention with neuroprotective or neuroenhancing therapies.

8.   Synaptic loss and electrophysiologic decline in glaucoma

Synaptic degeneration and changes in electrophysiology in the retina at RGC dendrites and in the brain at RGC axon terminals accompanies and indeed may even be part of the pathophysiology of RGC death and glaucoma progression. Thus, measuring the processing of visual stimuli in the retina and along the visual pathways in glaucoma may yield more reliable biomarkers than subjective visual function tests.

8.1.   Measuring RGC and retinal activity

Starting in the retina, the most commonly used variant of the pattern electroretinogram (pERG) records the retinal potential in response to contrast-reversal of patterned visual stimuli. The reversing stimulus helps average out photoreceptor and outer retinal signals, emphasizing inner retinal and RGC responses (Bach et al., 2013). Most often, pERGs are obtained using electrodes embedded in a corneal contact lens according to standards established by the International Society for Clinical Electrophysiology of Vision (ISCEV) (McCulloch et al., 2015; Robson et al., 2018). Studies of pERG in glaucoma report increased latency and reduced amplitude of the second negative wave (N-95) (May et al., 1982; Ringens et al., 1986; Trick et al., 1988; Weinstein et al., 1988) which is generated largely by RGCs (Bach et al., 2013). The pERG was reported helpful to discriminate between OHTN eyes that may develop glaucomatous visual field defects and those that probably will not in a long-term prospective study (Bach et al., 2006). In addition to predicting functional visual field defects, reduction in pERG amplitudes was reported to precede RNFL structural loss on the order of 8 years in glaucoma suspects (Banitt et al.,

2013). Although pERG may be helpful in detecting OHTN patients with high risk for glaucoma conversion, its utility in moderate to severe glaucoma is lost as the pERG signal is quickly lost in the noise as glaucoma progresses.

In contrast, the photopic negative response (PhNR) of the flash electroretinogram can be reliably detected in mild, moderate and severe glaucoma, showing improved recording ability in patients with poor cooperation and in eyes with imperfect media clarity without the need for refractive correction (Preiser et al., 2013). The PhNR is a negative wave elicited under light adapted conditions in response to brief flash stimuli that occurs after the positive b-wave. The full-field PhNR provides an objective measure of overall function of RGCs and their axons (Colotto et al., 2000; Viswanathan et al., 2001), and the ISCEV recently published an extended protocol for recording and analyzing the PhNR, including recommending long-wavelength (red) LED flash stimulus on a rod saturating short-wavelength (blue) background via dilated pupil to yield a large amplitude PhNR (Frishman et al., 2018). PhNR amplitudes correlate with glaucoma-induced clinical severity, degree of visual field defect and neural loss as assessed by structure of the ONH and RNFL (Machida et al., 2008, 2010, 2012). In addition, in glaucoma suspect eyes, a decrease in PhNR amplitude is associated with small changes in peripapillary retinal and macular NFL thicknesses (Cvenkel et al., 2017). However, a significant limitation of this modality is the considerable test–retest variability in PhNR amplitudes that is higher in glaucomatous eyes compared to normal eyes (Machida et al., 2008). We recently used PhNR as an exploratory endpoint in a prospective clinical trial of recombinant human nerve growth factor (clinicaltrials.gov #NCT02855450) and in preliminary analysis found the test-retest variability was very high (unpublished data). Because reproducibility declines further in eyes with low PhNR amplitudes, PhNR was not, in our hands, a suitable measure for observing the progression of the disease in patients with severe glaucoma, and it has not caught on as an outcome measure in larger long-term studies.

One particularly exciting new approach to imaging neuronal depolarization and action potentials leverages nanometer scale phase changes detected by OCT that may reflect cell membrane changes due to water movement associated with ionic shifts. Recent work using full-field ssOCT with computational aberration correction and clever phase referencing methods provided compelling measurements of photoreceptor path length changes after light stimulation with single cell transverse resolution. Recently, the same group has turned their promising technology to the GCL, with promising initial results, though the physiological origin of the inner retinal signals remains to be corroborated. These approaches, along with the possible translation of the use of functional dyes such as calcium or voltage indicators, commonly used in animal models but not yet transitioning to human testing, could prove to be very powerful biomarkers of impending glaucoma progression.

8.2. Advances in visual pathway electrophysiology

Beyond measuring RGC electrophysiology in the retina, and given the role of axon degeneration and dysfunction in the optic nerve and visual pathway, it is also motivating to study the complete visual pathway from eye to brain. The visual evoked potential (VEP) measures cortical activity associated with visual stimulus processing using electrodes placed

on the scalp (Odom et al., 2016). The utility of the VEP as a testing method in glaucoma was first documented decades ago when it was found that increases in pattern VEP latency were correlated with both the severity and location of visual field defects and the degree of cupping and pallor of the optic disc. Since that time, numerous other studies have documented sensitivity of the VEP to glaucomatous damage (Hood and Greenstein, 2003; Tai, 2018). The advantages of objective measurement and the correlation with visual filed test results suggest that the VEP could be a useful screening and follow-up tool in glaucoma.

However, despite promising data on VEP test modalities in the assessment of glaucoma, multiple aspects of test administration make their use challenging in a routine clinical setting. Such aspects include long test duration, the need for monitoring, and eliminating artifacts resulting from inattention or movement, as well as subjective waveform analysis and related issues with test-retest reliability. New VEP testing modalities such as short-duration transient VEP (SD-tVEP) and the isolated-check VEP (icVEP) allow VEP assessments to be performed more quickly and easily (Tai, 2018). SD-tVEP technology showed good within-session, inter-session repeatability, and good inter-eye correlation and agreement in normal subjects (Tello et al., 2010). In cases of asymmetric glaucoma, SD-tVEP was shown to correlate significantly with the level of HVF damage as measured by MD. In the eyes with more advanced HVF loss, reduced SD-tVEP amplitude was associated with decreased macular thickness on OCT (Plata et al., 2012). The correlations between MD and parameters of SD-tVEP were confirmed in a larger recent study (Waisbourd et al., 2017). icVEP on the other hand tests the function of the central retina using a matrix of small flickering targets and has a greater than 90% specificity in detecting visual function abnormalities in eyes with early-stage OAG (Fan et al., 2018), with a diagnostic power close to that of GCIPL analysis (Chen and Zhao, 2017b). An additional VEP subtype is the blue-on-yellow pattern stimulation VEP that was reported as a reliable tool to monitor for glaucoma progression as the peak times were significantly associated with progression of optic nerve damage (Horn et al., 2002). Lastly, the multifocal VEP (mfVEP) measures visual field by stimulating and recording signals from multiple discrete locations. The mfVEP is objective and comparable to HVF (Hood et al., 2004), but takes longer than HVF testing.

As discussed above, recent work in animal models of glaucoma has suggested that off-pathway function and structure are damaged first glaucoma (Della Santina et al., 2013; El-Danaf and Huberman, 2015; Ou et al., 2016; Puyang et al., 2017; Daniel et al., 2018). VEPs provide a possible means of measuring the response properties of the two pathways non-invasively using various types of incremental and decremental luminance modulation based on evidence that luminance decrements are preferentially processed by the off-pathway and vice versa. Specific assessment of on-versus off-pathway function with the VEP may thus be a sensitive indicator of early glaucoma. Several studies have compared VEP responses to contrast increments and decrements in healthy eyes (Zemon et al., 1988, 1995; Mutlukan et al., 1992; Roveri et al., 1997; Kremkow et al., 2014). Early studies of icVEPs used both sinusoidal increments and decrements (Zemon et al., 1988; Greenstein et al., 1998), but later work in glaucoma patients has used only incremental stimuli (Chen and Zhao, 2017a, 2017b; Xu et al., 2017; Fan et al., 2018). We have been studying sawtooth incremental and decremental luminance modulation, and our preliminary data suggest these produce differential responses in healthy controls (see Fig. 13). We are now studying whether

responses to decremental (off-pathway favoring) stimuli are more affected than incremental (ON pathway-favoring) stimuli in glaucoma patients, consistent with murine glaucoma models.

To summarize, although various types of VEP testing are available and adding an objective point of view to glaucoma diagnosis, the absence of larger studies for glaucoma, the technical aspects of signal recording and interpretation, as well as non-optimal specificity and sensitivity values, leaves the VEP as a non-mainstream clinical technology for glaucoma but as a potentially additive tool in questionable cases.

9. Deep learning in glaucoma

Improvements in glaucoma biomarker development are also expected to leverage the significant advances in the field of artificial intelligence (AI), and specifically in deep learning (DL). In glaucoma structure and function measures using fundus photographs, OCTs and HVFs, early data suggest DL algorithms provide high performance results for screening, diagnosis and progression detection, comparable to experienced human readers. For example, one DL algorithm trained on fundus images was found to detect referable glaucomatous optic neuropathy based on optic disc features with higher sensitivity and specificity, compared to eye care providers (Phene et al., 2019). In another study, a DL algorithm trained to quantify RNFL damage from fundus photographs performed at least as well as human graders at detecting eyes with repeatable glaucomatous visual field loss (Jammal et al., 2020). Similarly, a DL model using OCT measurement of macular RNFL showed promising results for early glaucoma diagnosis (Asaoka et al., 2019). A complete survey of this topic is beyond the scope of this paper but has received recent review elsewhere (Grewal et al., 2018; Ting et al., 2019a: Ting et al., 2019b). Challenges remain, including gathering adequately large and adequately annotated datasets. It is also interesting that DL algorithms may require orders of magnitude more data to train than humans to arrive at similar efficacy. The implications of this observation are as yet unknown. Nevertheless, the future of AI and DL applications in the field of glaucoma biomarker development is guaranteed to find utility and likely enter routine clinical use.

10. Molecular biomarkers

Molecular and cellular mechanisms involved in the initiation and propagation of neuronal injury of RGCs can be detected in body fluids and tissues, such as tear film, aqueous humor, vitreous body and blood serum. As discussed below, these may also provide better understanding of glaucoma pathophysiology and potentially identify candidate treatment targets for drug development.

10.1. Tear film

The tear film that covers the ocular surface can be readily sampled by Schirmer test papers or glass microcapillaries. It contains a large variety of proteins, some of which are hypothesized to be glaucoma- or drug-induced inflammatory molecules. For example, endothelin-1 (ET-1), a potent vasoactive peptide has been found in higher concentrations, in the tear film of patients with primary open-angle glaucoma (Pavlenko et al., 2013). ET-1

together with its precursor, big endothelin (bET), have been implicated in the regulation of IOP through modulation of the trabecular meshwork contractility that, in turn, affects aqueous humor outflow (Salvatore and Vingolo, 2010; Rosenthal and Fromm, 2011; Pavlenko et al., 2018), as well as through vasoconstriction that could reduce retinal blood flow (Salvatore and Vingolo, 2010; Rosenthal and Fromm, 2011).

Neurotrophic factors are a class of regulatory proteins that promote proliferation, differentiation, survival, and functioning of neurons (Pasquin et al., 2015). Numerous studies have shown the neuroprotective effect of CNTF) on RGCs (Flachsbarth et al., 2014). Moreover, the concentration of CNTF in the tear film and aqueous humor of patients with POAG has been shown to be inverse correlation with visual field loss, especially in those with severe visual field loss (Shpak et al., 2017). CNTF is a neurotrophic factor that participates in regulation of oxygen consumption, as discussed above. It is particularly interesting to consider reduced CNTF as a biomarker for glaucoma, as a phase 2 randomized clinical trial assessing CNTF as a therapy for glaucoma patients is currently underway (Clinicaltrials.gov #NCT02862938), highlighting the possible confluence of biomarker studies and therapeutic trials.

In glaucoma, several studies have emphasized the role of apoptotic factors, such as Fas ligand (FasL) in retinal neurotoxicity (Krishnan et al., 2019). FasL deficiency protects RGCs from cell death (Gregory et al., 2011), and there is an association of POAG onset and progression with interruption of FAS-mediated apoptosis (Slepova et al., 2012). Other studies have looked at immune signaling pathways as a factor in glaucomatous pathophysiology. An exploratory study including a number of cytokines and other immune system-related molecules documented altered tear film levels of lysozyme C, lipocalin-1, protein S100, immunoglobulins and prolactin-inducible protein in patients with medically treated POAG. Moreover, a differential pattern of phosphorylated cystatin-S distinguished POAG from healthy subjects and patients with pseudoexfoliative glaucoma (PEXG) (Pieragostino et al., 2012). Another study demonstrated significantly lower IL-12p70 levels in tear film of treatment-naïve glaucoma patients versus controls (Gupta et al., 2017).

Other biomarkers in the tear film may relate to IOP, RGC degeneration or the treatment of eye pressure. In one human subjects research study there was a higher level of kalikrein and angiotensin converting enzyme (ACE) activity measured in aqueous flow and tears, when comparing POAG to normal controls (Borovic et al., 2009). In animal studies, renin inhibitors, ACE inhibitors and angiotensin (1–7) lower IOP when locally administered (Holappa et al., 2015). These biomarkers may thus also be relevant to potentially therapeutic pathways.

Other tear-film biomarker studies have compared treated versus untreated patients. One well-designed longitudinal study found that a subgroup of 12 upregulated proteins in treatment-naive POAG patients were downregulated in patients whose IOP was controlled with prostaglandin analog (PGA) topical therapy (Pieragostino et al., 2013). These data raise the important question of whether biomarkers are disease- or treatment-emergent, particularly when studying surface inflammation known to be induced by topical glaucoma mediations. A number of studies have documented that the topical use of PGAs or other

topical medications result in changes to various inflammatory markers in the tear film, including metalloproteinases (MMP) and tissue metalloproteinases inhibitor, which may be triggered by inflammatory cytokines, resulting in an increase of matrix degradation and decrease of stromal collagens in the cornea (Lopilly Park et al., 2012); increased tear levels of S100-A8, S100-A9, mammaglobin B, and 14-3-3 ζ/δ (Wong et al., 2011); levels of IL-2, IL-5, IL-10, IL-12 (p70), IL-13, IL-15, IL-17, fibroblast growth factor basic, platelet-derived growth factor –BB, and tumor necrosis factor-α in patients receiving preserved latanoprost compared to normal controls (Martinez-de-la-Casa et al., 2017); and pro-inflammatory (IL1β, IL6, IL12, TNFα), T helper (Th)1 (INFγ, IL2) and Th2 (IL5, IL10, IL4) cytokines (Malvitte et al., 2007). These cytokines may carry signaling relevance to ocular surface pathology, as for example chemokine receptors in the conjunctival epithelium of glaucoma patients treated over the long term with various preserved topical anti-glaucoma drugs show increased expression, suggesting that the chronic use of topical treatments may stimulate both the Thl and Th2 immune response systems simultaneously (Baudouin et al., 2008).

Relatively fewer groups have investigated specific topical formulations directly, but a few studies have begun to address whether there are differences in drug or preservative effects. For example, comparing two PGAs directly, MMP-9 expression and tear cytokines involved in tissue remodeling were higher in eyes receiving latanoprost, whereas MMP-2 expression and cytokines regulating allergic pathways were higher in eyes receiving bimatoprost (Reddy et al., 2018). Interestingly, interleukin-1β expression was lower in glaucoma patients who received IOP-lowering eye drops without preservatives compared with those who received eye drops with preservatives (Benitez-Del-Castillo et al., 2019). Together these data suggest that while topical anti-glaucoma therapy may induce ocular surface inflammation, untangling effects of disease stabilization versus therapy side effects remains a challenge in interpreting such experiments. Broadly, tear film molecular expression in glaucoma patients may reveal promising pathogenesis-related, treatment-related or even pharmacogenetic-related biomarkers.

10.2. Aqueous humor biomarkers

Aqueous humor is the transparent fluid in the anterior and posterior chambers of the eye and is formed by the ciliary epithelium. Aqueous fluid and its circulation serves many functions, including distributing protein and non-protein nutrients and signaling molecules throughout the anterior segment, and in disease or infection, distributing immune cells and cytokines. It contains proteins secreted from anterior segment tissues (To et al., 2002), and total protein levels in aqueous humor are modified in many diseases affecting the anterior segment of the eye, including in POAG (Duan et al., 2008, 2010). Aqueous humor may contain markers directly related to or even derived from RGC neuro-degeneration, inflammation, immune response, and oxidative stress.

Multiple studies have reported differences between the aqueous humor proteome of POAG patients and controls. For example, aqueous humor levels of superoxide dismutase (SOD) as well as of glutathione transferase (GT) were significantly lower in glaucoma patients than controls, and both nitric oxide synthase and glutamine synthase (GS) expression were significantly higher among patients than controls. These data suggest the hypothesis that GS

overexpression might be related to neuronal injury and point to the potential role of glutamate as a modulator of ciliary body signaling, whereas the reduced expression of the antioxidant enzymes SOD and GT could aggravate an imbalance between oxygen- and nitrogen-derived free radical production and detoxification (Bagnis et al., 2012). In contrast with the above, in another study a significant increase in SOD and glutathione peroxidase (GPX) activities was found in aqueous humor of glaucoma patients in comparison to controls, suggesting that a significant increase in oxidative stress may play a role in the pathogenesis of glaucoma (Goyal et al., 2014). In parallel, low expression of SOD1 was found in the serum of glaucoma patients (Canizales et al., 2016), consistent with the reported proteomic levels in aqueous humor. Serum studies are discussed further below.

As the extracellular matrix (ECM) of the trabecular meshwork (TM) is important in regulating IOP in both normal and glaucomatous eyes, aqueous humor biomarkers that can regulate the TM's ECM proteins could link a marker to pathophysiology. For example, ECM composition and the TM actin cytoskeleton can be regulated by transforming growth factor TGF-β2, which was found in higher amounts in the aqueous humor of patients with POAG (Junglas et al., 2012). Furthermore, TGF-B2 concentrations are directly linked to the decreased ability of the TM to pass aqueous humor effectively, leading to elevation of IOP (Fuchshofer and Tamm, 2012). Besides the resulting in rise of IOP, TGF-β2 is also implicated in TM alteration by epithelial-to-mesenchymal transition and in ONH damage by tissue remodeling (Fuchshofer, 2011).

A number of studies have identified differential expression of cytokines and chemokines in the aqueous humor and the anterior chamber tissues of patients with POAG. For example, significantly increased levels of IL-8, TGF-β1, TNF-α and serum amyloid A were detected in aqueous humor of POAG and pseudoexfoliation glaucoma patients compared to senile cataract patient controls. These findings were consistent with similar findings of higher levels of IL-8 (Ten Beige et al., 2019) and other previous results (Kuchtey et al., 2010; Takai et al., 2012) including elevation of cytokines proportional to increasing IOP in POAG (Freedman and Iserovich, 2013) and in angle-closure patients (Huang et al., 2014) to a higher degree than chronic angle closure (Du et al., 2016). Disease staging may make a difference in the degree of biomarker or cytokine detection, as for example granulocyte colony-stimulating factor and monocyte chemotactic protein-1 levels were significantly different among different PACG disease stages (Wang et al., 2018). Together these data support the hypothesis that immune activation occurs in glaucoma.

Other molecular pathways have also been implicated by aqueous humor studies in glaucoma patients. In a recent study on the aqueous humor proteome, of 87 proteins found to be significantly different between glaucomatous and control aqueous humor (34 upregulated, and 53 downregulated), differentially expressed proteins were found to be involved in cholesterol- and proteolysis related pathways, in addition to inflammatory, metabolic, and antioxidant processes (Kaeslin et al., 2016). Overall, the significance and potential role as clinical biomarkers of different cytokines and other molecular alterations in aqueous humor of POAG patients as well as the relationship between cytokines, disease mechanism, IOP, medications and surgical intervention requires further investigation. However, because sampling the aqueous humor is invasive and is generally limited to patients undergoing an

intraocular surgery, its utility outside of research as a clinical diagnostic tool may require alternative non-invasive approaches such as imaging in the future.

10.3. Vitreous biomarkers

Although more invasive to sample and considerably less commonly approached surgically in glaucoma patients, the proximity of the vitreous to the RGCs makes it a more attractive target than the tear film or aqueous fluids. For example, one study demonstrated a twofold elevation in the level of glutamate in the vitreous body of the group of patients with glaucoma when compared with that in a control population (Dreyer et al., 1996). However, further study did not confirm these results (Honkanen et al., 2003). Looking at cytokine levels in the vitreous of glaucoma patients, vitreous levels of IL-2, IL-5, MCP-1, TNF-α and IP-10 were significantly higher in an acute angle closure glaucoma (AACG) group, indicating that inflammation and immune reaction have a strong link with the pathology of glaucoma, especially of AACG (Tong et al., 2017). In another study, about 5000 proteins were quantified from retinal tissue and vitreous fluid of glaucoma and control eyes (Mirzaei et al., 2017). Pathway analyses of differentially regulated proteins indicated defects in mitochondrial oxidative phosphorylation machinery and activation of classical complement pathway-associated proteins indicative of innate inflammatory response, consistent with biological pathways previously linked to glaucoma in animal models, for example (Howell et al., 2011; Takihara et al., 2015). Interestingly, of the differentially regulated proteins, 122 were found linked with pathophysiology of Alzheimer's disease (AD) (Mirzaei et al., 2017). Identification of previously reported and novel pathways in glaucoma that overlap with other CNS neurodegenerative disorders promises to provide renewed understanding of the etiology and pathogenesis of age-related neurodegenerative diseases.

Inadequate access to vitreous samples has and likely will continue to limit such studies in human glaucoma patients, although discoveries of vitreous biomarkers in animal models could focus subsequent human subject research on specific hypotheses, e.g. to search for specific molecules in the vitreous, aqueous, tear film or serum. For example, elevated IOP resulted in a 25-fold increase of catalase and 9-fold increase of X-linked inhibitor of apoptosis protein content in the vitreous compared to control eye in an experimental mouse model of glaucoma (Walsh et al., 2009). Studies integrating across animal models and human patients are likely to be a fruitful direction for future work.

10.4. Serum biomarkers

There are multiple avenues by which serum might reflect underlying RGC degeneration and thus serve as a biomarker or even reveal underlying pathophysiology of glaucoma. For example, RGC degeneration may lead to release of neuronal-specific proteins detectable in the bloodstream, or lead to changes in immune cell activation, which could also play a role in the pathophysiology of degeneration itself (Chen et al., 2018). Studies are beginning to explore such serum biomarkers, and their potential links to pathophysiology are indeed encouraging. For example, serum oxidative stress-related molecules were shown to be altered in glaucoma patients. Examining serum oxidation degradation products demonstrated that total antioxidant capacity and advanced oxidation protein products SOD and GPX were all found to be decreased, and malonyl dialdehyde, serine, transferrin, and vitamins A and E

increased in glaucoma patients (Engin et al., 2010). Given the potential role of vascular autoregulation in glaucoma, studies on serum levels of vascular tone-regulating molecules have aroused scientific curiosity as well. For instance, one study demonstrated that asymmetric dimethylarginine and symmetric dimethylarginine, isomeric derivatives of 1-arginine which act as endogenous NOS inhibitors, were found to be elevated in patients with advanced glaucoma (Javadiyan et al., 2012). Another study showed that endothelin-1 levels in glaucoma patients are on average 5 times higher than the corresponding median physiological concentration (Malishevskaia and Dolgova, 2014). In addition, plasma N-terminal proatrial natriuretic peptide (NT-proANP) concentration was increased in glaucoma patients compared to controls, and plasma and aqueous humor NT-proANP levels were correlated in glaucoma patients (Baumane et al., 2017), supporting the hypothesis that serum testing may reflect ocular pathophysiology.

As with intraocular fluid data, inflammatory pathway alterations have been uncovered in the peripheral serum of glaucoma patients. For example, significant alterations of serum TH1 and TH2 cytokines IL-4 and IL-6 were correlated to severity of glaucomatous optic neuropathy, along with a significant increase of serum IL-12p70 and a significant decrease in serum TNF-alpha levels compared to controls (Huang et al., 2010).

Another potentially related molecular network is the neurotrophin family, whose members could play an important role in neurodegener-ative diseases such as glaucoma and Alzheimer's. For example BDNF, a neurotrophic factor that participates in regulation of cerebral blood flow as discussed in 'Blood flow, oxygen, and metabolic dysregulation' section, is decreased in the aqueous humor, tear film, and peripheral blood serum of patients with early POAG and relatively increased in more advanced stages of the disease (Shpak et al., 2018). Neurotrophic factors have been studied extensively for therapeutic effect in glaucoma models in animals and are moving into clinical trials, as noted above, and thus carry potential for combined diagnostic and therapeutic investigation. Numerous metabolism- and cell cycle-related proteins such as citrate, connective tissue metabolism related molecules such as P I CP and P III NP, soluble fas (sFas)/Apo-1 and sFas ligand, and others are in various stages of investigation as well (Nath et al., 2017). As collection of blood samples is safe and minimally invasive procedure, serum glaucoma biomarkers, once established, may gain access into routine clinical use.

10.5. Molecular crossover with other optic neuropathies

Glaucoma likely shares cellular and molecular changes with other optic neuropathies such as ischemic or traumatic optic neuropathy and optic neuritis. Although the underlying pathophysiology of disease causation may differ in each optic neuropathy, in all of these, acute or progressive degeneration and death of RGCs may lead to shared or overlapping molecular changes detectable in the eye or serum. For example, a study evaluating prognostic biomarkers in optic neuritis, revealed that oligoclonal immunoglobulin G (IgG) bands predicted conversion to clinically definite MS after an optic neuritis episode (Tejeda-Velarde et al., 2018). Another study searched for vascular changes in Leber's hereditary optic neuropathy, finding significant peripapillary miscrovascular changes over the different stages of LHON, as a new imaging biomarker (Balducci et al., 2018). Thus, although shared

pathophysiology may confer some advantages in discovery of biomarkers, specificity across optic neuropathies may be limited in simple or single biomarkers, and the use of panels or more multiplexed molecular probes may ultimately be required for broad clinical value. It is important to note that this same issue will hold true for imaging- and electrophysiology-based candidate biomarkers discussed above.

11. Conclusions and future directions

Despite the existence of clinically adopted biomarkers for the diagnosis and treatment of glaucoma, the need for new biomarkers with higher sensitivity and specificity remains. This is particularly important for glaucoma as disease impact could be dramatically reduced through early diagnosis and improved management. Sensitive biomarkers of glaucoma progression could also reduce the duration of clinical trials, as well as improve the evaluation of efficacy through improved patient selection. In fact, clinical trials are already drawing exploratory imaging biomarkers into exploratory endpoints, and using molecular biomarkers to identify therapeutic candidates, such as NGF (ClinicalTrials.gov identifier: NCT02855450), CNTF (ClinicalTrials.gov identifier: NCT01949324), and anti-C1q (ClinicalTrials.gov identifier: NCT03010046). We anticipate that to serve these different unmet needs, different biomarkers will prove useful. Although formal validation of novel biomarkers for these purposes is expected to take years of longitudinal clinical testing in properly designed trials, we propose that merging biomarker testing as exploratory endpoints in therapeutic trials may accelerate their path to utility.

Acknowledgments

References

Abegão Pinto L, Willekens K, Van Keer K, Shibesh A, Molenberghs G, Vandewalle E, Stalmans I, 2016 Ocular blood flow in glaucoma - the Leuven eye study. Acta Ophthalmol. 94, 592–598. [PubMed: 26895610]

Agostinone J, Di Polo A, 2015 Retinal ganglion cell dendrite pathology and synapse loss: implications for glaucoma. Prog. Brain Res. 220, 199–216. [PubMed: 26497792]

Agostinone J, Alarcon-Martinez L, Gamlin C, Yu WQ, Wong ROL, Di Polo A, 2018 Insulin signalling promotes dendrite and synapse regeneration and restores circuit function after axonal injury. Brain 141, 1963–1980. [PubMed: 29931057]

Airaksinen PJ, Drance SM, Douglas GR, Mawson DK, Nieminen H, 1984 Diffuse and localized nerve fiber loss in glaucoma. Am. J. Ophthalmol. 98, 566–571. [PubMed: 6496612]

Alnawaiseh M, Lahme L, Muller V, Rosentreter A, Eter N, 2018 Correlation of flow density, as measured using optical coherence tomography angiography, with structural and functional parameters in glaucoma patients. Graefes Arch. Clin. Exp. Ophthalmol 256, 589–597. [PubMed: 29332249]

Armaly MF, 1970 Optic cup in normal and glaucomatous eyes. Invest. Ophthalmol 9, 425–429. [PubMed: 5446046]

Asaoka R, Murata H, Hirasawa K, Fujino Y, Matsuura M, Miki A, Kanamoto T, Ikeda Y, Mori K, Iwase A, Shoji N, Inoue K, Yamagami J, Araie M, 2019 Using Deep Learning and transform

learning to accurately diagnose early-onset glaucoma from macular optical coherence tomography images. Am. J. Ophthalmol 198, 136–145. [PubMed: 30316669]

Ashimatey BS, King BJ, Burns SA, Swanson WH, 2018a Evaluating glaucomatous abnormality in peripapillary optical coherence tomography enface visualisation of the retinal nerve fibre layer reflectance. Ophthalmic Physiol. Optic 38, 376–388.

Ashimatey BS, King BJ, Malinovsky VE, Swanson WH, 2018b Novel technique for quantifying retinal nerve fiber bundle abnormality in the temporal raphe. Optom. Vis. Sci 95, 309–317. [PubMed: 29561499]

Bach M, Unsoeld AS, Philippin H, Staubach F, Maier P, Walter HS, Bomer TG, Funk J, 2006 Pattern ERG as an early glaucoma indicator in ocular hypertension: a long-term, prospective study. Invest. Ophthalmol. Vis. Sci 47, 4881–4887. [PubMed: 17065502]

Bach M, Brigell MG, Hawlina M, Holder GE, Johnson MA, McCulloch DL, Meigen T, Viswanathan S, 2013 ISCEV standard for clinical pattern electroretinography (PERG): 2012 update. Doc. Ophthalmol 126, 1–7. [PubMed: 23073702]

Bagnis A, Izzotti A, Centofanti M, Sacca SC, 2012 Aqueous humor oxidative stress proteomic levels in primary open angle glaucoma. Exp. Eye Res 103, 55–62. [PubMed: 22974818]

Balducci N, Cascavilla ML, Ciardella A, La Morgia C, Triolo G, Parisi V, Bandello F, Sadun AA, Carelli V, Barboni P, 2018 Peripapillary vessel density changes in Leber's hereditary optic neuropathy: a new biomarker. Clin. Exp. Ophthalmol 46, 1055–1062. [PubMed: 29790285]

Banerjee D, Banerjee A, Mookherjee S, Vishal M, Mukhopadhyay A, Sen A, Basu A, Ray K, 2013 Mitochondrial genome analysis of primary open angle glaucoma patients. PloS One 8, e70760. [PubMed: 23940637]

Banitt MR, Ventura LM, Feuer WJ, Savatovsky E, Luna G, Shif O, Bosse B, Porciatti V, 2013 Progressive loss of retinal ganglion cell function precedes structural loss by several years in glaucoma suspects. Invest. Ophthalmol. Vis. Sci 54, 2346–2352. [PubMed: 23412088]

Baudouin C, Liang H, Hamard P, Riancho L, Creuzot-Garcher C, Warnet JM, Brignole-Baudouin F, 2008 The ocular surface of glaucoma patients treated over the long term expresses inflammatory markers related to both T-helper 1 and T-helper 2 pathways. Ophthalmology 115, 109–115. [PubMed: 17532048]

Baumane K, Ranka R, Laganovska G, 2017 Association of NT-proANP level in plasma and humor aqueous with primary open-angle glaucoma. Curr. Eye Res 42, 233–236. [PubMed: 27723368]

Baumann B, Potsaid B, Kraus MF, Liu JJ, Huang D, Hornegger J, Cable AE, Duker JS, Fujimoto JG, 2011 Total retinal blood flow measurement with ultrahigh speed swept source/Fourier domain OCT. Biomed. Optic Express 2, 1539–1552.

Benitez-Del-Castillo J, Cantu-Dibildox J, Sanz-Gonzalez SM, Zanon-Moreno V, Pinazo-Duran MD, 2019 Cytokine expression in tears of patients with glaucoma or dry eye disease: a prospective, observational cohort study. Eur. J. Ophthalmol 29, 437–443. [PubMed: 30175615]

Benson RC, Meyer RA, Zaruba ME, McKhann GM, 1979 Cellular autofluorescence–is it due to flavins? J. Histochem. Cytochem 27, 44–48. [PubMed: 438504]

Berdahl JP, Allingham RR, 2010 Intracranial pressure and glaucoma. Curr. Opin. Ophthalmol 21, 106–111. [PubMed: 20040876]

Berdahl JP, Fautsch MP, Stinnett SS, Allingham RR, 2008 Intracranial pressure in primary open angle glaucoma, normal tension glaucoma, and ocular hypertension: a case-control study. Invest. Ophthalmol. Vis. Sci 49, 5412–5418. [PubMed: 18719086]

Biomarkers Definitions Working, Group, 2001 Biomarkers and surrogate endpoints: preferred definitions and conceptual framework. Clin. Pharmacol. Ther 69, 89–95. [PubMed: 11240971]

Borovic D, Bendelic E, Chiselita D, 2009 [Study of kini-kallikrein and renin-angiotensin systems in patients with primary open angle glaucoma]. Oftalmologia 53, 61–68. [PubMed: 19697842]

Bourne RR, 2006 The optic nerve head in glaucoma. Community Eye Health 19, 44–45. [PubMed: 17491717]

Bowd C, Zangwill LM, Weinreb RN, Medeiros FA, Belghith A, 2017 Estimating optical coherence tomography structural measurement floors to improve detection of progression in advanced glaucoma. Am. J. Ophthalmol 175, 37–44. [PubMed: 27914978]

Brown A, 2003 Axonal transport of membranous and nonmembranous cargoes. J. Cell Biol 160, 817–821. [PubMed: 12642609]

Buckingham BP, Inman DM, Lambert W, Oglesby E, Calkins DJ, Steele MR, Vetter ML, Marsh-Armstrong N, Horner PJ, 2008 Progressive ganglion cell degeneration precedes neuronal loss in a mouse model of glaucoma. J. Neurosci 28, 2735–2744. [PubMed: 18337403]

Burgoyne CF, Downs JC, Bellezza AJ, Hart RT, 2004 Three-dimensional reconstruction of normal and early glaucoma monkey optic nerve head connective tissues. Invest. Ophthalmol. Vis. Sci 45, 4388–4399. [PubMed: 15557447]

Canizales L, Rodriguez L, Rivera C, Martinez A, Mendez F, Castillo A, 2016 Low-level expression of SOD1 in peripheral blood samples of patients diagnosed with primary open-angle glaucoma. Biomarkers Med. 10, 1218–1223.

Carbonelli M, La Morgia C, Savini G, Cascavilla ML, Borrelli E, Chicani F, do VF, Ramos C, Salomao SR, Parisi V, Sebag J, Bandello F, Sadun AA, Carelli V, Barboni P, 2015 Macular microcysts in mitochondrial optic neuropathies: prevalence and retinal layer thickness measurements. PloS One 10, e0127906. [PubMed: 26047507]

Cense B, Chen TC, Park BH, Pierce MC, de Boer JF, 2002 In vivo depth-resolved birefringence measurements of the human retinal nerve fiber layer by polarization-sensitive optical coherence tomography. Opt. Lett 27, 1610–1612. [PubMed: 18026517]

Cense B, Chen TC, Park BH, Pierce MC, de Boer JF, 2004 Thickness and birefringence of healthy retinal nerve fiber layer tissue measured with polarization-sensitive optical coherence tomography. Invest. Ophthalmol. Vis. Sci 45, 2606–2612. [PubMed: 15277483]

Cense B, Koperda E, Brown JM, Kocaoglu OP, Gao W, Jonnal RS, Miller DT, 2009 Volumetric retinal imaging with ultrahigh-resolution spectral-domain optical coherence tomography and adaptive optics using two broadband light sources. Optic Express 17, 4095–4111.

Chang EE, Goldberg JL, 2012 Glaucoma 2.0: neuroprotection, neuroregeneration, neuroenhancement. Ophthalmology 119, 979–986. [PubMed: 22349567]

Chang B, Smith RS, Hawes NL, Anderson MG, Zabaleta A, Savinova O, Roderick TH, Heckenlively JR, Davisson MT, John SW, 1999 Interacting loci cause severe iris atrophy and glaucoma in DBA/2J mice. Nat. Genet 21, 405–409. [PubMed: 10192392]

Chauhan BC, Burgoyne CF, 2013 From clinical examination of the optic disc to clinical assessment of the optic nerve head: a paradigm change. Am. J. Ophthalmol 156, 218–227. [PubMed: 23768651]

Chauhan BC, O'Leary N, AlMobarak FA, Reis ASC, Yang H, Sharpe GP, Hutchison DM, Nicolela MT, Burgoyne CF, 2013 Enhanced detection of open-angle glaucoma with an anatomically accurate optical coherence tomography-derived neuroretinal rim parameter. Ophthalmology 120, 535–543. [PubMed: 23265804]

Chen XW, Zhao YX, 2017a Comparison of isolated-check visual evoked potential and standard automated perimetry in early glaucoma and high-risk ocular hypertension. Int. J. Ophthalmol 10, 599–604. [PubMed: 28503434]

Chen X, Zhao Y, 2017b Diagnostic performance of isolated-check visual evoked potential versus retinal ganglion cell-inner plexiform layer analysis in early primary open-angle glaucoma. BMC Ophthalmol. 17, 77. [PubMed: 28532392]

Chen MF, Chui TY, Alhadeff P, Rosen RB, Ritch R, Dubra A, Hood DC, 2015a Adaptive optics imaging of healthy and abnormal regions of retinal nerve fiber bundles of patients with glaucoma. Invest. Ophthalmol. Vis. Sci 56, 674–681. [PubMed: 25574048]

Chen X, Kuehlewein L, Pineles SL, Tandon AK, Bose SX, Klufas MA, Sadda SR, Sarraf D, 2015b En face optical coherence tomography of macular microcysts due to optic neuropathy from neuromyelitis optica. Retin. Cases Brief Rep 9, 302–306. [PubMed: 26296052]

Chen H, Cho KS, Vu THK, Shen CH, Kaur M, Chen G, Mathew R, McHam ML, Fazelat A, Lashkari K, Au NPB, Tse JKY, Li Y, Yu H, Yang L, Stein-Streilein J, Ma CHE, Woolf CJ, Whary MT, Jager MJ, Fox JG, Chen J, Chen DF, 2018 Commensal microflora-induced T cell responses mediate progressive neurodegeneration in glaucoma. Nat. Commun 9, 3209. [PubMed: 30097565]

Chien JL, Ghassibi MP, Patthanathamrongkasem T, Abumasmah R, Rosman MS, Skaat A, Tello C, Liebmann JM, Ritch R, Park SC, 2017 Glaucoma diagnostic capability of global and regional

measurements of isolated ganglion cell layer and inner plexiform layer. J. Glaucoma 26, 208–215. [PubMed: 27811573]

Chong SP, Bernucci M, Radhakrishnan H, Srinivasan VJ, 2017 Structural and functional human retinal imaging with a fiber-based visible light OCT ophthalmoscope. Biomed. Optic Express 8, 323–337.

Chrysostomou V, Rezania F, Trounce IA, Crowston JG, 2013 Oxidative stress and mitochondrial dysfunction in glaucoma. Curr. Opin. Pharmacol 13, 12–15. [PubMed: 23069478]

Colotto A, Falsini B, Salgarello T, Iarossi G, Galan ME, Scullica L, 2000 Photopic negative response of the human ERG: losses associated with glaucomatous damage. Invest. Ophthalmol. Vis. Sci 41, 2205–2211. [PubMed: 10892864]

Cordeiro MF, Normando EM, Cardoso MJ, Miodragovic S, Jeylani S, Davis BM, Guo L, Ourselin S, A'Hern R, Bloom PA, 2017 Real-time imaging of single neuronal cell apoptosis in patients with glaucoma. Brain 140, 1757–1767. [PubMed: 28449038]

Crish SD, Sappington RM, Inman DM, Horner PJ, Calkins DJ, 2010 Distal axonopathy with structural persistence in glaucomatous neurodegeneration. Proc. Natl. Acad. Sci. U. S. A 107, 5196–5201. [PubMed: 20194762]

Cvenkel B, Sustar M, Perovsek D, 2017 Ganglion cell loss in early glaucoma, as assessed by photopic negative response, pattern electroretinogram, and spectral-domain optical coherence tomography. Doc. Ophthalmol 135, 17–28. [PubMed: 28567618]

Dai H, Yin D, Hu C, Morelli JN, Hu S, Yan X, Xu D, 2013a Whole-brain voxel-based analysis of diffusion tensor MRI parameters in patients with primary open angle glaucoma and correlation with clinical glaucoma stage. Neuroradiology 55, 233–243. [PubMed: 23223846]

Dai Y, Jonas JB, Huang H, Wang M, Sun X, 2013b Microstructure of parapapillary atrophy: beta zone and gamma zone. Invest. Ophthalmol. Vis. Sci 54, 2013–2018. [PubMed: 23462744]

Daniel S, Clark AF, McDowell CM, 2018 Subtype-specific response of retinal ganglion cells to optic nerve crush. Cell Death Dis. 4, 1–16.

Davis BM, Crawley L, Pahlitzsch M, Javaid F, Cordeiro MF, 2016 Glaucoma: the retina and beyond. Acta Neuropathol. 132, 807–826. [PubMed: 27544758]

de Boer JF, Hitzenberger CK, Yasuno Y, 2017 Polarization sensitive optical coherence tomography - a review [Invited]. Biomed. Optic Express 8, 1838–1873.

Della Santina L, Inman DM, Lupien CB, Horner PJ, Wong RO, 2013 Differential progression of structural and functional alterations in distinct retinal ganglion cell types in a mouse model of glaucoma. J. Neurosci 33, 17444–17457. [PubMed: 24174678]

Dmochowski JP, Greaves AS, Norcia AM, 2015 Maximally reliable spatial filtering of steady state visual evoked potentials. Neuroimage 109, 63–72. [PubMed: 25579449]

Doblhoff-Dier V, Schmetterer L, Vilser W, Garhofer G, Groschl M, Leitgeb RA, Werkmeister RM, 2014 Measurement of the total retinal blood flow using dual beam Fourier-domain Doppler optical coherence tomography with orthogonal detection planes. Biomed. Optic Express 5, 630–642.

Dong ZM, Wollstein G, Wang B, Schuman JS, 2017 Adaptive optics optical coherence tomography in glaucoma. Prog. Retin. Eye Res 57, 76–88. [PubMed: 27916682]

Dreyer EB, Zurakowski D, Schumer RA, Podos SM, Lipton SA, 1996 Elevated glutamate levels in the vitreous body of humans and monkeys with glaucoma. Arch. Ophthalmol 114, 299–305. [PubMed: 8600890]

Drucker E, Krapfenbauer K, 2013 Pitfalls and limitations in translation from biomarker discovery to clinical utility in predictive and personalised medicine. EPMA J. 4, 7. [PubMed: 23442211]

Du S, Huang W, Zhang X, Wang J, Wang W, Lam DSC, 2016 Multiplex cytokine levels of aqueous humor in acute primary angle-closure patients: fellow eye comparison. BMC Ophthalmol. 16, 6. [PubMed: 26748993]

Duan X, Lu Q, Xue P, Zhang H, Dong Z, Yang F, Wang N, 2008 Proteomic analysis of aqueous humor from patients with myopia. Mol. Vis 14, 370–377. [PubMed: 18334949]

Duan X, Xue P, Wang N, Dong Z, Lu Q, Yang F, 2010 Proteomic analysis of aqueous humor from patients with primary open angle glaucoma. Mol. Vis 16, 2839–2846. [PubMed: 21203405]

El-Danaf RN, Huberman AD, 2015 Characteristic patterns of dendritic remodeling in early-stage glaucoma: evidence from genetically identified retinal ganglion cell types. J. Neurosci 35, 2329–2343. [PubMed: 25673829]

El-Rafei A, Engelhorn T, Warntges S, Dorfler A, Hornegger J, Michelson G, 2011 A framework for voxel-based morphometric analysis of the optic radiation using diffusion tensor imaging in glaucoma. Magn. Reson. Imaging 29, 1076–1087. [PubMed: 21802876]

Engelhorn T, Michelson G, Waerntges S, Hempel S, El-Rafei A, Struffert T, Doerfler A, 2012 A new approach to assess intracranial white matter abnormalities in glaucoma patients: changes of fractional anisotropy detected by 3T diffusion tensor imaging. Acad. Radiol 19, 485–488. [PubMed: 22277635]

Engin KN, Yemisci B, Yigit U, Agachan A, Coskun C, 2010 Variability of serum oxidative stress biomarkers relative to biochemical data and clinical parameters of glaucoma patients. Mol. Vis 16, 1260–1271. [PubMed: 20664701]

Fan X, Wu LL, Di X, Ding T, Ding AH, 2018 Applications of isolated-check visual evoked potential in early stage of open-angle glaucoma patients. Chin. Med. J 131, 2439–2446. [PubMed: 30334529]

Field MG, Elner VM, Puro DG, Feuerman JM, Musch DC, Pop-Busui R, Hackel R, Heckenlively JR, Petty HR, 2008 Rapid, noninvasive detection of diabetes-induced retinal metabolic stress. Arch. Ophthalmol 126, 934–938. [PubMed: 18625939]

Field MG, Comer GM, Kawaji T, Petty HR, Elner VM, 2012 Noninvasive imaging of mitochondrial dysfunction in dry age-related macular degeneration. Ophthalmic Surg. Laser. Imag 43, 358–365.

Flachsbarth K, Kruszewski K, Jung G, Jankowiak W, Riecken K, Wagenfeld L, Richard G, Fehse B, Bartsch U, 2014 Neural stem cell-based intraocular administration of ciliary neurotrophic factor attenuates the loss of axotomized ganglion cells in adult mice. Invest. Ophthalmol. Vis. Sci 55, 7029–7039. [PubMed: 25270193]

Flammer J, 1994 The vascular concept of glaucoma. Surv. Ophthalmol 38, S3–S6. [PubMed: 7940146]

Freedman J, Iserovich P, 2013 Pro-inflammatory cytokines in glaucomatous aqueous and encysted Molteno implant blebs and their relationship to pressure. Invest. Ophthalmol. Vis. Sci 54, 4851–4855. [PubMed: 23788371]

Frishman L, Sustar M, Kremers J, McAnany JJ, Sarossy M, Tzekov R, Viswanathan S, 2018 ISCEV extended protocol for the photopic negative response (PhNR) of the full-field electroretinogram. Doc. Ophthalmol 136, 207–211. [PubMed: 29855761]

Fry LE, Fahy E, Chrysostomou V, Hui F, Tang J, van Wijngaarden P, Petrou S, Crowston JG, 2018 The coma in glaucoma: retinal ganglion cell dysfunction and recovery. Prog. Retin. Eye Res 65, 77–92. [PubMed: 29631042]

Fu CT, Sretavan DW, 2012 Ectopic vesicular glutamate release at the optic nerve head and axon loss in mouse experimental glaucoma. J. Neurosci 32,15859–15876. [PubMed: 23136425]

Fuchshofer R, 2011 The pathogenic role of transforming growth factor-beta2 in glaucomatous damage to the optic nerve head. Exp. Eye Res 93, 165–169. [PubMed: 20708611]

Fuchshofer R, Tamm ER, 2012 The role of TGF-beta in the pathogenesis of primary open-angle glaucoma. Cell Tissue Res. 347, 279–290. [PubMed: 22101332]

Gardiner SK, Ren R, Yang H, Fortune B, Burgoyne CF, Demirel S, 2014 A method to estimate the amount of neuroretinal rim tissue in glaucoma: comparison with current methods for measuring rim area. Am. J. Ophthalmol 157, 540–549. [PubMed: 24239775]

Gardiner SK, Demirel S, Reynaud J, Fortune B, 2016 Changes in retinal nerve fiber layer reflectance intensity as a predictor of functional progression in glaucoma. Invest. Ophthalmol. Vis. Sci 57, 1221–1227. [PubMed: 26978028]

Garhofer G, Zawinka C, Resch H, Huemer KH, Schmetterer L, Dorner GT, 2004 Response of retinal vessel diameters to flicker stimulation in patients with early open angle glaucoma. J. Glaucoma 13, 340–344. [PubMed: 15226664]

Geiger LK, Kortuem KR, Alexejun C, Levin LA, 2002 Reduced redox state allows prolonged survival of axotomized neonatal retinal ganglion cells. Neuroscience 109, 635–642. [PubMed: 11823072]

Geyman LS, Suwan Y, Garg R, Field MG, Krawitz BD, Mo S, Pinhas A, Ritch R, Rosen RB, 2018 Noninvasive detection of mitochondrial dysfunction in ocular hypertension and primary open-angle glaucoma. J. Glaucoma 27, 592–599. [PubMed: 29750714]

Gotzinger E, Pircher M, Baumann B, Hirn C, Vass C, Hitzenberger CK, 2008 Retinal nerve fiber layer birefringence evaluated with polarization sensitive spectral domain OCT and scanning laser polarimetry: a comparison. J. Biophot 1, 129–139.

Goyal A, Srivastava A, Sihota R, Kaur J, 2014 Evaluation of oxidative stress markers in aqueous humor of primary open angle glaucoma and primary angle closure glaucoma patients. Curr. Eye Res 39, 823–829. [PubMed: 24912005]

Greenstein VC, Seliger S, Zemon V, Ritch R, 1998 Visual evoked potential assessment of the effects of glaucoma on visual subsystems. Vision Res. 38, 1901–1911. [PubMed: 9797966]

Gregory MS, Hackett CG, Abernathy EF, Lee KS, Saff RR, Hohlbaum AM, Moody KS, Hobson MW, Jones A, Kolovou P, Karray S, Giani A, John SW, Chen DF, Marshak-Rothstein A, Ksander BR, 2011 Opposing roles for membrane bound and soluble Fas ligand in glaucoma-associated retinal ganglion cell death. PloS One 6, el7659.

Grewal PS, Oloumi F, Rubin U, Tennant MTS, 2018 Deep learning in ophthalmology: a review. Can. J. Ophthalmol 53, 309–313. [PubMed: 30119782]

Gugleta K, Fuchsjager-Mayrl G, Orgul S, 2007 Is neurovascular coupling of relevance in glaucoma? Surv. Ophthalmol 52 (Suppl. 2), S139–S143. [PubMed: 17998039]

Gugleta K, Kochkorov A, Waldmann N, Polunina A, Katamay R, Flammer J, Orgul S, 2012 Dynamics of retinal vessel response to flicker light in glaucoma patients and ocular hypertensives. Graefes Arch. Clin. Exp. Ophthalmol 250, 589–594. [PubMed: 22008947]

Gugleta K, Turksever C, Polunina A, Orgul S, 2013a Effect of ageing on the retinal vascular responsiveness to flicker light in glaucoma patients and in ocular hypertension. Br. J. Ophthalmol 97, 848–851. [PubMed: 23624271]

Gugleta K, Waldmann N, Polunina A, Kochkorov A, Katamay R, Flammer J, Orgul S, 2013b Retinal neurovascular coupling in patients with glaucoma and ocular hypertension and its association with the level of glaucomatous damage. Graefes Arch. Clin. Exp. Ophthalmol 251, 1577–1585. [PubMed: 23417339]

Gupta N, Greenberg G, de Tilly LN, Gray B, Polemidiotis M, Yu cel YH, 2009 Atrophy of the lateral geniculate nucleus in human glaucoma detected by magnetic resonance imaging. Br. J. Ophthalmol 93, 56–60. [PubMed: 18697810]

Gupta D, Wen JC, Huebner JL, Stinnett S, Kraus VB, Tseng HC, Walsh M, 2017 Cytokine biomarkers in tear film for primary open-angle glaucoma. Clin. Ophthalmol 11, 411–416. [PubMed: 28260854]

Harper RA, Reeves BC, 1999 Glaucoma screening: the importance of combining test data. Optom. Vis. Sci 76, 537–543. [PubMed: 10472959]

Hasegawa T, Akagi T, Yoshikawa M, Suda K, Yamada H, Kimura Y, Nakanishi H, Miyake M, Unoki N, Ikeda Hanako O., Yoshimura N, 2015 Microcystic inner nuclear layer changes and retinal nerve fiber layer defects in eyes with glaucoma. PloS One 10, e0130175. [PubMed: 26066021]

Hawker MJ, Vernon SA, Ainsworth G, Hillman JG, MacNab HK, Dua HS, 2005 Asymmetry in optic disc morphometry as measured by heidelberg retina tomography in a normal elderly population: the Bridlington Eye Assessment Project. Invest. Ophthalmol. Vis. Sci 46, 4153–4158. [PubMed: 16249493]

Hill BG, Dranka BP, Zou L, Chatham JC, Darley-Usmar VM, 2009 Importance of the bioenergetic reserve capacity in response to cardiomyocyte stress induced by 4-hydroxynonenal. Biochem. J 424, 99–107. [PubMed: 19740075]

Holappa M, Valjakka J, Vaajanen A, 2015 Angiotensin(l-7) and ACE2, "The hot spots" of renin-angiotensin system, detected in the human aqueous humor. Open Ophthalmol. J 9, 28–32. [PubMed: 25926900]

Hollo G, 2018 Optical coherence tomography angiography in glaucoma. Turk. J. Ophthalmol 48, 196–201. [PubMed: 30202616]

Honkanen RA, Baruah S, Zimmerman MB, Khanna CL, Weaver YK, Narkiewicz J, Waziri R, Gehrs KM, Weingeist TA, Boldt HC, Folk JC, Russell SR, Kwon YH, 2003 Vitreous amino acid concentrations in patients with glaucoma undergoing vitrectomy. Arch. Ophthalmol 121, 183–188. [PubMed: 12583783]

Hood DC, 2017 Improving our understanding, and detection, of glaucomatous damage: an approach based upon optical coherence tomography (OCT). Prog. Retin. Eye Res 57, 46–75. [PubMed: 28012881]

Hood DC, Greenstein VC, 2003 Multifocal VEP and ganglion cell damage: applications and limitations for the study of glaucoma. Prog. Retin. Eye Res 22, 201–251. [PubMed: 12604058]

Hood DC, Thienprasiddhi P, Greenstein VC, Winn BJ, Ohri N, Liebmann JM, Ritch R, 2004 Detecting early to mild glaucomatous damage: a comparison of the multifocal VEP and automated perimetry. Invest. Ophthalmol. Vis. Sci 45, 492–498. [PubMed: 14744890]

Hood DC, Chen MF, Lee D, Epstein B, Alhadeff P, Rosen RB, Ritch R, Dubra A, Chui TYP, 2015a Confocal adaptive optics imaging of peripapillary nerve fiber bundles: implications for glaucomatous damage seen on circumpapillary OCT scans. Transl. Vis. Sci. Technol 4, 12.

Hood DC, Fortune B, Mavrommatis MA, Reynaud J, Ramachandran R, Ritch R, Rosen RB, Muhammad H, Dubra A, Chui TY, 2015b Details of glaucomatous damage are better seen on OCT en face images than on OCT retinal nerve fiber layer thickness maps. Invest. Ophthalmol. Vis. Sci 56, 6208–6216. [PubMed: 26426403]

Hood DC, Lee D, Jarukasetphon R, Nunez J, Mavrommatis MA, Rosen RB, Ritch R, Dubra A, Chui TYP, 2017 Progression of local glaucomatous damage near fixation as seen with adaptive optics imaging. Transl. Vis. Sci. Technol 6, 6.

Horn FK, Jonas JB, Budde WM, Junemann AM, Mardin CY, Korth M, 2002 Monitoring glaucoma progression with visual evoked potentials of the blue-sensitive pathway. Invest. Ophthalmol. Vis. Sci 43, 1828–1834. [PubMed: 12036986]

Howell GR, Macalinao DG, Sousa GL, Walden M, Soto I, Kneeland SC, Barbay JM, King BL, Marchant JK, Hibbs M, Stevens B, Barres BA, Clark AF, Libby RT, John SW, 2011 Molecular clustering identifies complement and endothelin induction as early events in a mouse model of glaucoma. J. Clin. Invest 121, 1429–1444. [PubMed: 21383504]

Howell GR, Soto I, Libby RT, John SW, 2013 Intrinsic axonal degeneration pathways are critical for glaucomatous damage. Exp. Neurol 246, 54–61. [PubMed: 22285251]

Hoyt WF, Frisen L, Newman NM, 1973 Fundoscopy of nerve fiber layer defects in glaucoma. Invest. Ophthalmol 12, 814–829. [PubMed: 4752920]

Huang XR, Knighton RW, 2005 Microtubules contribute to the birefringence of the retinal nerve fiber layer. Invest. Ophthalmol. Vis. Sci 46, 4588–4593. [PubMed: 16303953]

Huang P, Qi Y, Xu YS, Liu J, Liao D, Zhang SS, Zhang C, 2010 Serum cytokine alteration is associated with optic neuropathy in human primary open angle glaucoma. J. Glaucoma 19, 324–330. [PubMed: 19730118]

Huang XR, Zhou Y, Kong W, Knighton RW, 2011 Reflectance decreases before thickness changes in the retinal nerve fiber layer in glaucomatous retinas. Invest. Ophthalmol. Vis. Sci 52, 6737–6742. [PubMed: 21730345]

Huang XR, Knighton RW, Zhou Y, Zhao XP, 2013 Reflectance speckle of retinal nerve fiber layer reveals axonal activity. Invest. Ophthalmol. Vis. Sci 54, 2616–2623. [PubMed: 23532525]

Huang W, Chen S, Gao X, Yang M, Zhang J, Li X, Wang W, Zhou M, Zhang X, Zhang X, 2014 Inflammation-related cytokines of aqueous humor in acute primary angle-closure eyes. Invest. Ophthalmol. Vis. Sci 55, 1088–1094. [PubMed: 24474267]

Hwang JC, Konduru R, Zhang X, Tan O, Francis BA, Varma R, Sehi M, Greenfield DS, Sadda SR, Huang D, 2012 Relationship among visual field, blood flow, and neural structure measurements in glaucoma. Invest. Ophthalmol. Vis. Sci 53, 3020–3026. [PubMed: 22447865]

Ivers KM, Sredar N, Patel NB, Rajagopalan L, Queener HM, Twa MD, Harwerth RS, Porter J, 2015 In vivo changes in lamina cribrosa microarchitecture and optic nerve head structure in early experimental glaucoma. PloS One 10, e0134223. [PubMed: 26230993]

Jammal AA, Thompson AC, Mariottoni EB, Berchuck SI, Urata CN, Estrela T, Wakil SM, Costa VP, Medeiros FA, 2020 Human versus machine: comparing a deep learning algorithm to human gradings for detecting glaucoma on fundus photographs. Am. J. Ophthalmol 211, 123–131. [PubMed: 31730838]

Javadiyan S, Burdon KP, Whiting MJ, Abhary S, Straga T, Hewitt AW, Mills RA, Craig JE, 2012 Elevation of serum asymmetrical and symmetrical dimethylarginine in patients with advanced glaucoma. Invest. Ophthalmol. Vis. Sci 53, 1923–1927. [PubMed: 22395885]

Jia Y, Morrison JC, Tokayer J, Tan O, Lombardi L, Baumann B, Lu CD, Choi W, Fujimoto JG, Huang D, 2012a Quantitative OCT angiography of optic nerve head blood flow. Biomed. Optic Express 3, 3127–3137.

Jia Y, Tan O, Tokayer J, Potsaid B, Wang Y, Liu JJ, Kraus MF, Subhash H, Fujimoto JG, Hornegger J, Huang D, 2012b Split-spectrum amplitude-decorrelation angiography with optical coherence tomography. Optic Express 20, 4710–4725.

Jia Y, Wei E, Wang X, Zhang X, Morrison JC, Parikh M, Lombardi LH, Gattey DM, Armour RL, Edmunds B, Kraus MF, Fujimoto JG, Huang D, 2014 Optical coherence tomography angiography of optic disc perfusion in glaucoma. Ophthalmology 121, 1322–1332. [PubMed: 24629312]

Jian Y, Lee S, Ju MJ, Heisler M, Ding W, Zawadzki RJ, Bonora S, Sarunic MV, 2016 Lens-based wavefront sensorless adaptive optics swept source OCT. Sci. Rep 6, 27620. [PubMed: 27278853]

Jung JH, Park JH, Yoo C, Kim YY, 2018 Localized retinal nerve fiber layer defects in red-free photographs versus en face structural optical coherence tomography images. J. Glaucoma 27, 269–274. [PubMed: 29303874]

Junglas B, Kuespert S, Seleem AA, Struller T, Ullmann S, Bosl M, Bosserhoff A, Kostler J, Wagner R, Tamm ER, Fuchshofer R, 2012 Connective tissue growth factor causes glaucoma by modifying the actin cytoskeleton of the trabecular mesh work. Am. J. Pathol 180, 2386–2403. [PubMed: 22542845]

Kaeslin MA, Killer HE, Fuhrer CA, Zeleny N, Huber AR, Neutzner A, 2016 Changes to the aqueous humor proteome during glaucoma. PloS One 11, e0165314. [PubMed: 27788204]

Kashani AH, Chen CL, Gahm JK, Zheng F, Richter GM, Rosenfeld PJ, Shi Y, Wang RK, 2017 Optical coherence tomography angiography: a comprehensive review of current methods and clinical applications. Prog. Retin. Eye Res 60, 66–100. [PubMed: 28760677]

Kasi A, Faiq MA, Chan KC, 2019 In vivo imaging of structural, metabolic and functional brain changes in glaucoma. Neural Regen. Res 14, 446–449. [PubMed: 30539811]

Khanifar AA, Parlitsis GJ, Ehrlich JR, Aaker GD, D'Amico DJ, Gauthier SA, Kiss S, 2010 Retinal nerve fiber layer evaluation in multiple sclerosis with spectral domain optical coherence tomography. Clin. Ophthalmol 4, 1007–1013. [PubMed: 20922034]

Kho A, Srinivasan VJ, 2019 Compensating spatially dependent dispersion in visible light OCT. Opt. Lett 44, 775–778. [PubMed: 30767984]

Kim HJ, Lee SY, Park Ki H., Kim DM, Jeoung JW, 2016 Glaucoma diagnostic ability of layer-by-layer segmented ganglion cell complex by spectral-domain optical coherence tomography. Invest. Ophthalmol. Vis. Sci 57, 4799–4805. [PubMed: 27654408]

Kim EK, Park HL, Park CK, 2017a Segmented inner plexiform layer thickness as a potential biomarker to evaluate open-angle glaucoma: dendritic degeneration of retinal ganglion cell. PloS One 12, e0182404. [PubMed: 28771565]

Kim YK, Ha A, Na KI, Kim HJ, Jeoung JW, Park KH, 2017b Temporal relation between macular ganglion cell-inner plexiform layer loss and peripapillary retinal nerve fiber layer loss in glaucoma. Ophthalmology 124, 1056–1064. [PubMed: 28408038]

Kim YN, Shin JW, Sung KR, 2018 Relationship between progressive changes in lamina cribrosa depth and deterioration of visual field loss in glaucomatous eyes. Kor. J. Ophthalmol 32, 470–477.

Kindzelskii A, Petty HR, 2004 Fluorescence spectroscopic detection of mitochondrial flavoprotein redox oscillations and transient reduction of the NADPH oxidase-associated flavoprotein in leukocytes. Eur. Biophys. J 33, 291–299. [PubMed: 14574524]

Kitsos G, Zikou AK, Bagli E, Kosta P, Argyropoulou MI, 2009 Conventional MRI and magnetisation transfer imaging of the brain and optic pathway in primary open-angle glaucoma. Br. J. Radiol 82, 896–900. [PubMed: 19433483]

Kiyota N, Kunikata H, Shiga Y, Omodaka K, Nakazawa T, 2018 Ocular microcirculation measurement with laser speckle flowgraphy and optical coherence tomography angiography in glaucoma. Acta Ophthalmol. 96, e485–e492. [PubMed: 29575676]

Kocaoglu OP, Cense B, Jonnal RS, Wang Q, Lee S, Gao W, Miller DT, 2011 Imaging retinal nerve fiber bundles using optical coherence tomography with adaptive optics. Vision Res. 51, 1835–1844. [PubMed: 21722662]

Kocaoglu OP, Turner TL, Liu Z, Miller DT, 2014 Adaptive optics optical coherence tomography at 1 MHz. Biomed. Optic Express 5, 4186–4200.

Kong GY, Van Bergen NJ, Trounce IA, Crowston JG, 2009 Mitochondrial dysfunction and glaucoma. J. Glaucoma 18, 93–100. [PubMed: 19225343]

Koontz MA, Hendrickson AE, 1987 Stratified distribution of synapses in the inner plexiform layer of primate retina. J. Comp. Neurol 263, 581–592. [PubMed: 3667989]

Kortuem K, Geiger LK, Levin LA, 2000 Differential susceptibility of retinal ganglion cells to reactive oxygen species. Invest. Ophthalmol. Vis. Sci 41, 3176–3182. [PubMed: 10967081]

Kremkow J, Jin J, Komban SJ, Wang Y, Lashgari R, Li X, Jansen M, Zaidi Q, Alonso JM, 2014 Neuronal nonlinearity explains greater visual spatial resolution for darks than lights. Proc. Natl. Acad. Sci. U. S. A 111, 3170–3175. [PubMed: 24516130]

Krishnan A, Kocab AJ, Zacks DN, Marshak-Rothstein A, Gregory-Ksander M, 2019 A small peptide antagonist of the Fas receptor inhibits neuroinflammation and prevents axon degeneration and retinal ganglion cell death in an inducible mouse model of glaucoma. J. Neuroinflammation 16, 184. [PubMed: 31570110]

Kuchtey J, Rezaei KA, Jaru-Ampornpan P, Sternberg P Jr., Kuchtey RW, 2010 Multiplex cytokine analysis reveals elevated concentration of interleukin-8 in glaucomatous aqueous humor. Invest. Ophthalmol. Vis. Sci 51, 6441–6447. [PubMed: 20592224]

Kuehn MH, Fingert JH, Kwon YH, 2005 Retinal ganglion cell death in glaucoma: mechanisms and neuroprotective strategies. Ophthalmol. Clin 18, 383–395.

Kurokawa K, Liu Z, Crowell J, Zhang F, Miller DT, 2018 Method to investigate temporal dynamics of ganglion and other retinal cells in the living human eye. In: Proc. SPIE Ophthalmic Technologies, XXVIII, 10474, 104740W.

Lagreze WA, Gaggl M, Weigel M, Schulte-Monting J, Buhler A, Bach M, Munk RD, Bley TA, 2009 Retrobulbar optic nerve diameter measured by high-speed magnetic resonance imaging as a biomarker for axonal loss in glaucomatous optic atrophy. Invest. Ophthalmol. Vis. Sci 50, 4223–4228. [PubMed: 19407026]

Laslandes M, Salas M, Hitzenberger CK, Pircher M, 2017 Increasing the field of view of adaptive optics scanning laser ophthalmoscopy. Biomed. Optic Express 8, 4811–4826.

Lavinsky F, Wu M, Schuman JS, Lucy KA, Liu M, Song Y, Fallon J, de Los Angeles Ramos Cadena M, Ishikawa H, Wollstein G, 2018 Can macula and optic nerve head parameters detect glaucoma progression in eyes with advanced circumpapillary retinal nerve fiber layer damage? Ophthalmology 125, 1907–1912. [PubMed: 29934267]

Leitgeb RA, Werkmeister RM, Blatter C, Schmetterer L, 2014 Doppler optical coherence tomography. Prog. Retin. Eye Res 41, 26–43. [PubMed: 24704352]

Lim H, Mujat M, Kerbage C, Lee EC, Chen Y, Chen TC, de Boer JF, 2006 High-speed imaging of human retina in vivo with swept-source optical coherence tomography. Optic Express 14, 12902–12908.

Lin C, Mak H, Yu M, Leung C, 2017 Trend-based progression analysis for examination of the topography of rates of retinal nerve fiber layer thinning in glaucoma. JAMA Ophthalmol. 135, 189–195. [PubMed: 28152147]

Liu T, Wei Q, Wang J, Jiao S, Zhang HF, 2011 Combined photoacoustic microscopy and optical coherence tomography can measure metabolic rate of oxygen. Biomed. Optic Express 2, 1359–1365.

Liu S, Wang B, Yin B, Milner TE, Markey MK, McKinnon SJ, Rylander HG 3rd, 2014 Retinal nerve fiber layer reflectance for early glaucoma diagnosis. J. Glaucoma 23, e45–e52. [PubMed: 23835671]

Liu L, Jia Y, Takusagawa HL, Pechauer AD, Edmunds B, Lombardi L, Davis E, Morrison JC, Huang D, 2015 Optical coherence tomography angiography of the peripapillary retina in glaucoma. JAMA ophthalmol. 133, 1045–1052. [PubMed: 26203793]

Liu Z, Kurokawa K, Zhang F, Lee JJ, Miller DT, 2017 Imaging and quantifying ganglion cells and other transparent neurons in the living human retina. Proc. Natl. Acad. Sci. U. S. A 114, 12803–12808. [PubMed: 29138314]

Liu Z, Tam J, Saeedi O, Hammer DX, 2018 Trans-retinal cellular imaging with multimodal adaptive optics. Biomed. Optic Express 9, 4246–4262.

Lopilly Park HY, Kim JH, Lee KM, Park CK, 2012 Effect of prostaglandin analogues on tear proteomics and expression of cytokines and matrix metalloproteinases in the conjunctiva and cornea. Exp. Eye Res 94, 13–21. [PubMed: 22067128]

Machida S, 2012 Clinical applications of the photopic negative response to optic nerve and retinal diseases. J. Ophthalmol 2012, 397178. [PubMed: 23133741]

Machida S, Gotoh Y, Toba Y, Ohtaki A, Kaneko M, Kurosaka D, 2008 Correlation between photopic negative response and retinal nerve fiber layer thickness and optic disc topography in glaucomatous eyes. Invest. Ophthalmol. Vis. Sci 49, 2201–2207. [PubMed: 18436853]

Machida S, Tamada K, Oikawa T, Yokoyama D, Kaneko M, Kurosaka D, 2010 Sensitivity and specificity of photopic negative response of focal electoretinogram to detect glaucomatous eyes. Br. J. Ophthalmol 94, 202–208. [PubMed: 19692386]

Malishevskaia TN, Dolgova IG, 2014 [Options for correction of endothelial dysfunction and oxidative stress in patients with primary open-angle glaucoma]. Vestn. Oftalmol 130 (67–70), 72–73.

Malvitte L, Montange T, Vejux A, Baudouin C, Bron AM, Creuzot-Garcher C, Lizard G, 2007 Measurement of inflammatory cytokines by multi cytokine assay in tears of patients with glaucoma topically treated with chronic drugs. Br. J. Ophthalmol 91, 29–32. [PubMed: 16943231]

Marcic TS, Belyea DA, Katz B, 2003 Neuroprotection in glaucoma: a model for neuroprotection in optic neuropathies. Curr. Opin. Ophthalmol 14, 353–356. [PubMed: 14615639]

Martinez A, Sanchez M, 2005 Predictive value of colour Doppler imaging in a prospective study of visual field progression in primary open-angle glaucoma. Acta Ophthalmol. Scand 83, 716–722. [PubMed: 16396650]

Martinez-de-la-Casa JM, Perez-Bartolome F, Urcelay E, Santiago JL, Moreno-Montanes J, Arriola-Villalobos P, Benitez-Del-Castillo JM, Garcia-Feijoo J, 2017 Tear cytokine profile of glaucoma patients treated with preservative-free or preserved latanoprost. Ocul. Surf 15, 723–729. [PubMed: 28342814]

May JG, Ralston JV, Reed JL, Van Dyk HJ, 1982 Loss in pattern-elicited electroretinograms in optic nerve dysfunction. Am. J. Ophthalmol 93, 418–422. [PubMed: 7072808]

McCulloch DL, Marmor MF, Brigell MG, Hamilton R, Holder GE, Tzekov R, Bach M, 2015 ISCEV Standard for full-field clinical electroreti no graphy (2015 update). Doc. Ophthalmol 130, 1–12.

Miguel AIM, Silva AB, Azevedo LF, 2019 Diagnostic performance of optical coherence tomography angiography in glaucoma: a systematic review and meta-analysis. Br. J. Ophthalmol 103, 1677–1684. [PubMed: 30728123]

Mirzaei M, Gupta VB, Chick JM, Greco TM, Wu Y, Chitranshi N, Wall RV, Hone E, Deng L, Dheer Y, Abbasi M, Rezaeian M, Braidy N, You Y, Salekdeh GH, Haynes PA, Molloy MP, Martins R, Cristea IM, Gygi SP, Graham SL, Gupta VK, 2017 Age-related neurodegenerative disease associated pathways identified in retinal and vitreous proteome from human glaucoma eyes. Sci. Rep 7, 12685. [PubMed: 28978942]

Moghimi S, Fatehi N, Nguyen AH, Romero P, Caprioli J, Nouri-Mahdavi K, 2019 Relationship of the macular ganglion cell and inner plexiform layers in healthy and glaucoma eyes. Transl. Vis. Sci. Technol 8, 27.

Mokhtari M, Rabbani H, Mehri-Dehnavi A, Kafieh R, Akhlaghi MR, Pourazizi M, Fang L, 2019 Local comparison of cup to disc ratio in right and left eyes based on fusion of color fundus images and OCT B-scans. Inf. Fusion 51, 30–41.

Mozaffarieh M, Grieshaber MC, Flammer J, 2008 Oxygen and blood flow: players in the pathogenesis of glaucoma. Mol. Vis 14, 224–233. [PubMed: 18334938]

Mroczkowska S, Benavente-Perez A, Negi A, Sung V, Patel SR, Gherghel D, 2013 Primary open-angle glaucoma vs normal-tension glaucoma: the vascular perspective. JAMA Ophthalmol. 131, 36–43. [PubMed: 22964974]

Mujat M, Lu Y, Maguluri G, Zhao Y, Iftimia N, Ferguson RD, 2019 Visualizing the vasculature of the entire human eye posterior hemisphere without a contrast agent. Biomed. Optic Express 10, 167–180.

Murphy MC, Conner IP, Teng CY, Lawrence JD, Safiullah Z, Wang B, Bilonick RA, Kim SG, Wollstein G, Schuman JS, Chan KC, 2016 Retinal structures and visual cortex activity are impaired prior to clinical vision loss in glaucoma. Sci. Rep 6, 31464. [PubMed: 27510406]

Mursch-Edlmayr AS, Luff N, Podkowinski D, Ring M, Schmetterer L, Bolz M, 2018 Laser speckle flowgraphy derived characteristics of optic nerve head perfusion in normal tension glaucoma and healthy individuals: a Pilot study. Sci. Rep 8, 5343. [PubMed: 29593269]

Mutlukan E, Bradnam M, Keating D, Damato BE, 1992 Visual evoked cortical potentials from transient dark and bright stimuli. Selective 'on' and 'off-pathway' testing? Doc. Ophthalmol 80, 171–181. [PubMed: 1425132]

Mwanza JC, Budenz DL, Warren JL, Webel AD, Reynolds CE, Barbosa DT, Lin S, 2015 Retinal nerve fibre layer thickness floor and corresponding functional loss in glaucoma. Br. J. Ophthalmol 99, 732–737. [PubMed: 25492547]

Na JH, Sung KR, Lee JR, Lee KS, Baek S, Kim HK, Sohn YH, 2013 Detection of glaucomatous progression by spectral-domain optical coherence tomography. Ophthalmology 120, 1388–1395. [PubMed: 23474248]

Nadler Z, Wang B, Schuman JS, Ferguson RD, Patel A, Hammer DX, Bilonick RA, Ishikawa H, Kagemann L, Sigal IA, Wollstein G, 2014 In vivo three-dimensional characterization of the healthy human lamina cribrosa with adaptive optics spectral-domain optical coherence tomography. Invest. Ophthalmol. Vis. Sci 55, 6459–6466. [PubMed: 25228539]

Nath M, Haider N, Velpandian T, 2017 Circulating biomarkers in glaucoma, age-related macular degeneration, and diabetic retinopathy. Indian J. Ophthalmol 65, 191–197. [PubMed: 28440247]

O'Connor Daniel J., Zeyen Thierry, Caprioli Joseph, 1993 Comparisons of methods to detect glaucomatous optic nerve damage. Ophthalmology 100, 1498–1503. [PubMed: 8414410]

Odom JV, Bach M, Brigell M, Holder GE, McCulloch DL, Mizota A, Tormene AP, International Society for Clinical Electrophysiology of Vision, 2016. ISCEV standard for clinical visual evoked potentials: (2016 update). Doc. Ophthalmol 133, 1–9.

Olafsdottir OB, Hardarson SH, Gottffedsdottir MS, Harris A, Stefansson E, 2011 Retinal oximetry in primary open-angle glaucoma. Invest. Ophthalmol. Vis. Sci 52, 6409–6413. [PubMed: 21715353]

Olafsdottir OB, Vandewalle E, Abegao Pinto L, Geirsdottir A, De Clerck E, Stalmans P, Gottffedsdottir MS, Kristjansdottir JV, Van Calster J, Zeyen T, Stefansson E, Stalmans I, 2014 Retinal oxygen metabolism in healthy subjects and glaucoma patients. Br. J. Ophthalmol 98, 329–333. [PubMed: 24403567]

Omodaka K, Horii T, Takahashi S, Kikawa T, Matsumoto A, Shiga Y, Maruyama K, Yuasa T, Akiba M, Nakazawa T, 2015 3D evaluation of the lamina cribrosa with swept-source optical coherence tomography in normal tension glaucoma. PloS One 10, e0122347. [PubMed: 25875096]

Ong LS, Mitchell P, Healey PR, Cumming RG, 1999 Asymmetry in optic disc parameters: the blue mountains eye study. Invest. Ophthalmol. Vis. Sci 40, 849–857. [PubMed: 10102281]

Orgul S, 2007 Blood flow in glaucoma. Br. J. Ophthalmol 91, 3–5. [PubMed: 17179119]

Ou Y, Jo RE, Ullian EM, Wong RO, Della Santina L, 2016 Selective vulnerability of specific retinal ganglion cell types and synapses after transient ocular hypertension. J. Neurosci 36, 9240–9252. [PubMed: 27581463]

Pasquin S, Sharma M, Gauchat JF, 2015 Ciliary neurotrophic factor (CNTF): new facets of an old molecule for treating neurodegenerative and metabolic syndrome pathologies. Cytokine Growth Factor Rev. 26, 507–515. [PubMed: 26187860]

Pavlenko TA, Chesnokova NB, Davydova HG, Okhotsimskaia TD, Beznos OV, Grigor'ev AV, 2013 [Level of tear endothelin-1 and plasminogen in patients with glaucoma and proliferative diabetic retinopathy]. Vestn. Oftalmol 129, 20–23.

Pavlenko TA, Kim AR, Kurina AY, Davydova NG, Kolomojceva EM, Chesnokova NB, Ugrumov MV, 2018 [Endothelins and dopamine levels in tears for assessment of neurovascular disorders in glaucoma]. Vestn. Oftalmol 134, 41–46.

Phene S, Dunn RC, Hammel N, Liu Y, Krause J, Kitade N, Schaekermann M, Sayres R, Wu DJ, Bora A, Semturs C, Misra A, Huang AE, Spitze A, Medeiros FA, Maa AY, Gandhi M, Corrado GS, Peng L, Webster DR, 2019 Deep learning and glaucoma specialists: the relative importance of

optic disc features to predict glaucoma referral in fundus photographs. Ophthalmology 126, 1627–1639. [PubMed: 31561879]

Pieragostino D, Bucci S, Agnifili L, Fasanella V, D'Aguanno S, Mastropasqua A, Ciancaglini M, Mastropasqua L, Di Ilio C, Sacchetta P, Urbani A, Del Boccio P, 2012 Differential protein expression in tears of patients with primary open angle and pseudoexfoliative glaucoma. Mol. Biosyst 8, 1017–1028. [PubMed: 22124706]

Pieragostino D, Agnifili L, Fasanella V, D'Aguanno S, Mastropasqua R, Di Hio C, Sacchetta P, Urbani A, Del Boccio P, 2013 Shotgun proteomics reveals specific modulated protein patterns in tears of patients with primary open angle glaucoma naive to therapy. Mol. Biosyst 9, 1108–1116. [PubMed: 23580065]

Pircher M, Zawadzki RJ, 2017 Review of adaptive optics OCT (AO-OCT): principles and applications for retinal imaging Invited. Biomed. Optic Express 8, 2536–2562.

Potsaid B, Gorczynska I, Srinivasan VJ, Chen Y, Jiang J, Cable A, Fujimoto JG, 2008 Ultrahigh speed spectral/Fourier domain OCT ophthalmic imaging at 70,000 to 312,500 axial scans per second. Optic Express 16, 15149–15169.

Prata TS, Lima VC, De Moraes CG, Trubnik V, Derr P, Liebmann JM, Ritch R, Tello C, 2012 Short duration transient visual evoked potentials in glaucomatous eyes. J. Glaucoma 21, 415–420. [PubMed: 21562431]

Preiser D, Lagreze WA, Bach M, Poloschek CM, 2013 Photopic negative response versus pattern electroreti nogram in early glaucoma. Invest. Ophthalmol. Vis. Sci 54, 1182–1191. [PubMed: 23307968]

Price DA, Grzybowski A, Eikenberry J, Januleviciene I, Verticchio V, Alice C, Mathew S, Siesky B, Harris A, 2019 Review of non-invasive intracranial pressure measurement techniques for ophthalmology applications, pii: bjophthalmol-2019-314704 Br. J. Ophthalmol. 10.1136/bjophthalmol-2019-314704 [Epub ahead of print].

Puyang Z, Gong HQ, He SG, Troy JB, Liu X, Liang PJ, 2017 Different functional susceptibilities of mouse retinal ganglion cell subtypes to optic nerve crush injury. Exp. Eye Res 162, 97–103. [PubMed: 28629926]

Quigley HA, Flower RW, Addicks EM, McLeod DS, 1980a The mechanism of optic nerve damage in experimental acute intraocular pressure elevation. Invest. Ophthalmol. Vis. Sci 19, 505–517. [PubMed: 6154668]

Quigley HA, Miller NR, George T, 1980b Clinical evaluation of nerve fiber layer atrophy as an indicator of glaucomatous optic nerve damage. Arch. Ophthalmol 98, 1564–1571. [PubMed: 7425916]

Quigley HA, Katz J, Derick RJ, Gilbert D, Sommer A, 1992 An evaluation of optic disc and nerve fiber layer examinations in monitoring progression of early glaucoma damage. Ophthalmology 99, 19–28. [PubMed: 1741133]

Radius RL, Anderson DR, 1981 Rapid axonal transport in primate optic nerve. Distribution of pressure-induced interruption. Arch. Ophthalmol 99, 650–654. [PubMed: 6164358]

Ramakrishan R, Krishnadas R, Robin AL, Khurana M, 2013 Diagnosis and Management of Glaucoma. New Delhi, India.

Raza AS, Hood DC, 2015 Evaluation of the structure-function relationship in glaucoma using a novel method for estimating the number of retinal ganglion cells in the human retina. Invest. Ophthalmol. Vis. Sci 56, 5548–5556. [PubMed: 26305526]

Razeen MM, Steven S, Sredar N, Cheong SK, Yarp J, Nuñez M, Goldberg JL, Dubra A, 2018 High resolution imaging of inner retinal microcystic changes in glaucoma In: The Association for Research in Vision and Ophthalmology. Hawaii, USA.

Reddy S, Sahay P, Padhy D, Sarangi S, Suar M, Modak R, Rao A, 2018 Tear biomarkers in latanoprost and bimatoprost treated eyes. PloS One 13, e0201740. [PubMed: 30080906]

Reinert KC, Dunbar RL, Gao W, Chen G, Ebner TJ, 2004 Flavoprotein autofluorescence imaging of neuronal activation in the cerebellar cortex in vivo. J. Neurophysiol 92, 199–211. [PubMed: 14985415]

Rilvén S, Torp TL, Grauslund J, 2017 Retinal oximetry in patients with ischaemic retinal diseases. Acta Ophthalmol. 95, 119–127. [PubMed: 27585711]

Ringens PJ, Vijfvinkel-Bruinenga S, van Lith GH, 1986 The pattern-elicited electroretinogram. I. A tool in the early detection of glaucoma? Ophthalmologica 192, 171–175. [PubMed: 3725315]

Riva C, Ross B, Benedek GB, 1972 Laser Doppler measurements of blood flow in capillary tubes and retinal arteries. Invest. Ophthalmol 11, 936–944. [PubMed: 4634958]

Riva CE, Geiser M, Petrig BL, 2010 Ocular blood flow assessment using continuous laser Doppler flowmetry. Acta Ophthalmol. 88, 622–629. [PubMed: 19860779]

Robson AG, Nilsson J, Li S, Jalali S, Fulton AB, Tormene AP, Holder GE, Brodie SE, 2018 ISCEV guide to visual electrodiagnostic procedures. Doc. Ophthalmol 136, 1–26.

Rosenthal R, Fromm M, 2011 Endothelin antagonism as an active principle for glaucoma therapy. Br. J. Pharmacol 162, 806–816. [PubMed: 21054341]

Rossi EA, Granger CE, Sharma R, Yang Q, Saito K, Schwarz C, Walters S, Nozato K, Zhang J, Kawakami T, Fischer W, Latchney LR, Hunter JJ, Chung MM, Williams DR, 2017 Imaging individual neurons in the retinal ganglion cell layer of the living eye. Proc. Natl. Acad. Sci. U. S. A 114, 586–591. [PubMed: 28049835]

Roveri L, Demarco PJ Jr., Celesia GG, 1997 An electrophysiological metric of activity within the ON- and OFF-pathways in humans. Vision Res. 37, 669–674. [PubMed: 9156211]

Saleh A, Roy Chowdhury SK, Smith DR, Balakrishnan S, Tessler L, Martens C, Morrow D, Schartner E, Frizzi KE, Calcutt NA, Fernyhough P, 2013 Ciliary neurotrophic factor activates NF-kappaB to enhance mitochondrial bioenergetics and prevent neuropathy in sensory neurons of streptozotocin-induced diabetic rodents. Neuropharmacology 65, 65–73. [PubMed: 23022047]

Salvatore S, Vingolo EM, 2010 Endothelin-1 role in human eye: a review. J. Ophthalmol 2010, 354645. [PubMed: 21461356]

Schuman JS, Hee MR, Arya AV, Pedut-Kloizman T, Puliafito CA, Fujimoto JG, Swanson EA, 1995a Optical coherence tomography: a new tool for glaucoma diagnosis. Curr. Opin. Ophthalmol 6, 89–95. [PubMed: 10150863]

Schuman JS, Hee MR, Puliafito CA, Wong C, Pedut-Kloizman T, Lin CP, Hertzmark E, Izatt JA, Swanson EA, Fujimoto JG, 1995b Quantification of nerve fiber layer thickness in normal and glaucomatous eyes using optical coherence tomography. Arch. Ophthalmol 113, 586–596. [PubMed: 7748128]

Scoles D, Sulai YN, Dubra A, 2013 In vivo dark-field imaging of the retinal pigment epithelium cell mosaic. Biomed. Optic Express 4, 1710–1723.

Scoles D, Higgins BP, Cooper RF, Dubis AM, Summerfelt P, Weinberg DV, Kim JE, Stepien KE, Carroll J, Dubra A, 2014 Microscopic inner retinal hyper-reflective phenotypes in retinal and neurologic disease. Invest. Ophthalmol. Vis. Sci 55, 4015–4029. [PubMed: 24894394]

Sehi M, Goharian I, Konduru R, Tan O, Srinivas S, Sadda SR, Francis BA, Huang D, Greenfield DS, 2014 Retinal blood flow in glaucomatous eyes with single-hemifield damage. Ophthalmology 121, 750–758. [PubMed: 24290800]

Shibuki K, Hishida R, Murakami H, Kudoh M, Kawaguchi T, Watanabe M, Watanabe S, Kouuchi T, Tanaka R, 2003 Dynamic imaging of somatosensory cortical activity in the rat visualized by flavoprotein autofluorescence. J. Physiol 549, 919–927. [PubMed: 12730344]

Shpak AA, Guekht AB, Druzhkova TA, Kozlova KI, Gulyaeva NV, 2017 Ciliary neurotrophic factor in patients with primary open-angle glaucoma and age-related cataract. Mol. Vis 23, 799–809. [PubMed: 29225456]

Shpak AA, Guekht AB, Druzhkova TA, Kozlova KI, Gulyaeva NV, 2018 Brain-derived neurotrophic factor in patients with primary open-angle glaucoma and age-related cataract. Curr. Eye Res 43, 224–231. [PubMed: 29120253]

Shu X, Beckmann L, Zhang H, 2017 Visible-light optical coherence tomography: a review. J. Biomed. Optic 22, 1–14.

Shughoury A, Mathew S, Arciero J, Wurster P, Adjei S, Ciulla T, Siesky B, Harris A, 2020 Retinal oximetry in glaucoma: investigations and findings reviewed. Acta Ophthalmol. 10.1111/aos.14397. Online ahead of print.

Siaudvytyte L, Januleviciene I, Ragauskas A, Bartusis L, Siesky B, Harris A, 2015 Update in intracranial pressure evaluation methods and translaminar pressure gradient role in glaucoma. Acta Ophthalmol. 93, 9–15. [PubMed: 25043873]

Siesky B, Harris A, Kagemann L, Stefansson E, McCranor L, Miller B, Bwatwa J, Regev G, Ehrlich R, 2010 Ocular blood flow and oxygen delivery to the retina in primary open-angle glaucoma patients: the addition of dorzolamide to timolol monotherapy. Acta Ophthalmol. 88, 142–149. [PubMed: 19706018]

Sigal IA, Wang B, Strouthidis NG, Akagi T, Girard MJ, 2014 Recent advances in OCT imaging of the lamina cribrosa. Br. J. Ophthalmol 98 (Suppl. 2), ii34–ii39. [PubMed: 24934221]

Slepova OS, Frolov MA, Morozova NS, Frolov AM, Lovpache DN, 2012 [Markers of Fas-mediated apoptosis in primary open-angle glaucoma and opportunities of their pharmacological correction]. Vestn. Oftalmol 128, 27–31.

Sommer A, Miller NR, Pollack I, Maumenee AE, George T, 1977 The nerve fiber layer in the diagnosis of glaucoma. Arch. Ophthalmol 95, 2149–2156. [PubMed: 588106]

Sommer A, Quigley HA, Robin AL, Miller NR, Katz J, Arkell S, 1984 Evaluation of nerve fiber layer assessment. Arch. Ophthalmol 102, 1766–1771. [PubMed: 6508617]

Sommer A, Katz J, Quigley HA, et al., 1991a Clinically detectable nerve fiber atrophy precedes the onset of glaucomatous field loss. Arch. Ophthalmol 109, 77–83. [PubMed: 1987954]

Sommer A, Tielsch JM, Katz J, Quigley HA, Gottsch JD, Javitt J, Singh K, 1991b Relationship between intraocular pressure and primary open angle glaucoma among white and black Americans. Arch. Ophthalmol 109, 1090–1095. The Baltimore Eye Survey. [PubMed: 1867550]

Song W, Wei Q, Liu W, Liu T, Yi J, Sheibani N, Fawzi AA, Linsenmeier RA, Jiao S, Zhang HF, 2014 A combined method to quantify the retinal metabolic rate of oxygen using photoacoustic ophthalmoscopy and optical coherence tomography. Sci. Rep 4, 6525. [PubMed: 25283870]

Srinivasan VJ, Huber R, Gorczynska I, Fujimoto JG, Jiang JY, Reisen P, Cable AE, 2007 High-speed, high-resolution optical coherence tomography retinal imaging with a frequency-swept laser at 850 nm. Opt. Lett 32, 361–363. [PubMed: 17356653]

Srinivasan VJ, Adler DC, Chen Y, Gorczynska I, Huber R, Duker JS, Schuman JS, Fujimoto JG, 2008 Ultrahigh-speed optical coherence tomography for three-dimensional and en face imaging of the retina and optic nerve head. Invest. Ophthalmol. Vis. Sci 49, 5103–5110. [PubMed: 18658089]

Srinivasan VJ, Sakadzic S, Gorczynska I, Ruvinskaya S, Wu W, Fujimoto JG, Boas DA, 2010 Quantitative cerebral blood flow with optical coherence tomography. Optic Express 18, 2477–2494.

Srinivasan VJ, Radhakrishnan H, Lo EH, Mandeville ET, Jiang JY, Barry S, Cable AE, 2012 OCT methods for capillary velocimetry. Biomed. Optic Express 3, 612–629.

Stevens B, Allen NJ, Vazquez LE, Howell GR, Christopherson KS, Nouri N, Micheva KD, Mehalow AK, Huberman AD, Stafford B, Sher A, Litke AM, Lambris JD, Smith SJ, John SW, Barres BA, 2007 The classical complement cascade mediates CNS synapse elimination. Cell 131, 1164–1178. [PubMed: 18083105]

Strimbu K, Tavel JA, 2010 What are biomarkers? Curr. Opin. HIV AIDS 5, 463–466. [PubMed: 20978388]

Sugiyama T, Araie M, Riva CE, Schmetterer L, Orgul S, 2010 Use of laser speckle flowgraphy in ocular blood flow research. Acta Ophthalmol. 88, 723–729. [PubMed: 19725814]

Sung KR, Na JH, Lee Y, 2012 Glaucoma diagnostic capabilities of optic nerve head parameters as determined by Cirrus HD optical coherence tomography. J. Glaucoma 21, 498–504. [PubMed: 21637115]

Swanson WH, King BJ, Burns SA, 2019 Within-subject variability in human retinal nerve fiber bundle width. PloS One 14, e0223350. [PubMed: 31618224]

Szkulmowski M, Gorczynska I, Szlag D, Sylwestrzak M, Kowalczyk A, Wojtkowski M, 2012 Efficient reduction of speckle noise in optical coherence tomography. Optic Express 20, 1337–1359.

Tai TYT, 2018 Visual evoked potentials and glaucoma. Asia Pac. J. Ophthalmol 7, 352–355.

Takai Y, Tanito M, Ohira A, 2012 Multiplex cytokine analysis of aqueous humor in eyes with primary open-angle glaucoma, exfoliation glaucoma, and cataract. Invest. Ophthalmol. Vis. Sci 53, 241–247. [PubMed: 22159018]

Takayama K, Ooto S, Hangai M, Arakawa N, Oshima S, Shibata N, Hanebuchi M, Inoue T, Yoshimura N, 2012 High-resolution imaging of the retinal nerve fiber layer in normal eyes using adaptive optics scanning laser ophthalmoscopy. PloS One 7, e33158. [PubMed: 22427978]

Takeyama A, Ishida K, Anraku A, Ishida M, Tomita G, 2018 Comparison of optical coherence tomography angiography and laser speckle flowgraphy for the diagnosis of normal-tension glaucoma. J. Ophthalmol 2018, 1751857. [PubMed: 29651339]

Takihara Y, Inatani M, Eto K, Inoue T, Kreymerman A, Miyake S, Ueno S, Nagaya M, Nakanishi Ayami I, Keiichiro T, Yoshihiro S, Hirotaka S, Keita K, Mineo S, Tatsuya, Goldberg JL, Nabekura J, Tanihara H, 2015 In vivo imaging of axonal transport of mitochondria in the diseased and aged mammalian CNS. Proc. Natl. Acad. Sci 112, 10515–10520. [PubMed: 26240337]

Tan O, Liu L, Zhang X, Morrison JC, Huang D, 2016 Glaucoma increases retinal surface contour variability as measured by optical coherence tomography. Invest. Ophthalmol. Vis. Sci 57, OCT438–OCT443. [PubMed: 27409503]

Tanna H, Dubis AM, Ayub N, Tait DM, Rha J, Stepien KE, Carroll J, 2010 Retinal imaging using commercial broadband optical coherence tomography. Br. J. Ophthalmol 94, 372–376. [PubMed: 19770161]

Tejeda-Velarde A, Costa-Frossard L, Sainz de la Maza S, Carrasco A, Espino M, Picon C, Toboso I, Walo PE, Lourido D, Muriel A, Alvarez-Cermeno JC, Villar LM, 2018 Clinical usefulness of prognostic biomarkers in optic neuritis. Eur. J. Neurol 25, 614–618. [PubMed: 29272057]

Tello C, De Moraes CG, Prata TS, Derr P, Patel J, Siegfried J, Liebmann JM, Ritch R, 2010 Repeatability of short-duration transient visual evoked potentials in normal subjects. Doc. Ophthalmol 120, 219–228. [PubMed: 20111979]

Ten Berge JC, Fazil Z, van den Born I, Wolfs RCW, Schreurs Dik, W.A., Rothova A, 2019 Intraocular cytokine profile and autoimmune reactions in retinitis pigmentosa, age-related macular degeneration, glaucoma and cataract. Acta Ophthalmol. 97, 185–192. [PubMed: 30298670]

Tezel G, Wax MB, 2004 Hypoxia-inducible factor 1alpha in the glaucomatous retina and optic nerve head. Arch. Ophthalmol 122, 1348–1356. [PubMed: 15364715]

Ting DSW, Pasquale LR, Peng L, Campbell JP, Lee AY, Raman R, Tan GSW, Schmetterer L, Keane PA, Wong TY, 2019a Artificial intelligence and deep learning in ophthalmology. Br. J. Ophthalmol 103, 167–175. [PubMed: 30361278]

Ting DSW, Peng L, Varadarajan AV, Keane PA, Burlina P, Chiang MF, Schmetterer L, Pasquale LR, Bressler NM, Webster DR, Abramoff M, Wong TY, 2019b Deep learning in ophthalmology: the technical and clinical considerations. Prog. Retin. Eye Res 72, 100759. [PubMed: 31048019]

To CH, Kong CW, Chan CY, Shahidullah M, Do CW, 2002 The mechanism of aqueous humour formation. Clin. Exp. Optom 85, 335–349. [PubMed: 12452784]

Tong Y, Zhou YL, Zheng Y, Biswal M, Zhao PQ, Wang ZY, 2017 Analyzing cytokines as biomarkers to evaluate severity of glaucoma. Int. J. Ophthalmol 10, 925–930. [PubMed: 28730084]

Torti C, Považay B, Hofer B, Unterhuber A, Carroll J, Ahnelt PK, Drexler W, 2009 Adaptive optics optical coherence tomography at 120,000 depth scans/s for non-invasive cellular phenotyping of the living human retina. Optic Express 17, 19382–19400.

Trick GL, Bickler-Bluth M, Cooper DG, Kolker AE, Nesher R, 1988 Pattern reversal electroretinogram (PRERG) abnormalities in ocular hypertension: correlation with glaucoma risk factors. Curr. Eye Res 7, 201–206. [PubMed: 3371068]

Vandewalle E, Abegao Pinto L, Olafsdottir OB, De Clerck E, Stalmans P, Van Calster J, Zeyen T, Stefansson E, Stalmans I, 2014 Oximetry in glaucoma: correlation of metabolic change with structural and functional damage. Acta Ophthalmol. 92, 105–110. [PubMed: 23323611]

van der Schoot J, Vermeer KA, de Boer JF, Lemij HG, 2012 The effect of glaucoma on the optical attenuation coefficient of the retinal nerve fiber layer in spectral domain optical coherence tomography images. Invest. Ophthalmol. Vis. Sci 53, 2424–2430. [PubMed: 22427540]

Ventura LM, Porciatti V, 2006 Pattern electroreti nogram in glaucoma. Curr. Opin. Ophthalmol 17, 196–202. [PubMed: 16552256]

Vilupuru AS, Rangaswamy NV, Frishman LJ, Smith EL 3rd, Harwerth RS, Roorda A, 2007 Adaptive optics scanning laser ophthalmoscopy for in vivo imaging of lamina cribrosa. J. Opt. Soc. Am. Optic Image Sci. Vis 24, 1417–1425.

Viswanathan S, Frishman LJ, Robson JG, Walters JW, 2001 The photopic negative response of the flash electroreti nogram in primary open angle glaucoma. Invest. Ophthalmol. Vis. Sci 42, 514–522. [PubMed: 11157891]

Waisbourd M, Gensure RH, Aminlari A, Shah SB, Khanna N, Sood N, Molineaux J, Gonzalez A, Myers JS, Katz LJ, 2017 Short-duration transient visual evoked potentials and color reflectivity discretization analysis in glaucoma patients and suspects. Int. J. Ophthalmol 10, 254–261. [PubMed: 28251085]

Walsh MM, Yi H, Friedman J, Cho KI, Tserentsoodol N, McKinnon S, Searle K, Yeh A, Ferreira PA, 2009 Gene and protein expression pilot profiling and biomarkers in an experimental mouse model of hypertensive glaucoma. Exp. Biol. Med 234, 918–930.

Wang LC, Chiang MC, Chen L, Chang CJ, Liao CY, 2003 Performance comparisons of power allocation mechanisms for downlink handoff in the WCDMA system with microcellular environments. In: The Sixth ACM international workshop on modeling, analysis and simulation of wireless and mobile systems, 2–10. San Diego CA USA, Sep. 2003.

Wang Y, Bower BA, Izatt JA, Tan O, Huang D, 2008 Retinal blood flow measurement by circumpapillary Fourier domain Doppler optical coherence tomography. J. Biomed. Optic 13, 064003.

Wang Y, Fawzi A, Tan O, Gil-Flamer J, Huang D, 2009a Retinal blood flow detection in diabetic patients by Doppler Fourier domain optical coherence tomography. Optic Express 17, 4061–4073.

Wang Y, Lu A, Gil-Flamer J, Tan O, Izatt JA, Huang D, 2009b Measurement of total blood flow in the normal human retina using Doppler Fourier-domain optical coherence tomography. Br. J. Ophthalmol 93, 634–637. [PubMed: 19168468]

Wang B, Nevins JE, Nadler Z, Wollstein G, Ishikawa H, Bilonick RA, Kagemann L, Sigal IA, Grulkowski I, Liu JJ, Kraus M, Lu CD, Hornegger J, Fujimoto JG, Schuman JS, 2013 In vivo lamina cribrosa micro-architecture in healthy and glaucomatous eyes as assessed by optical coherence tomography. Invest. Ophthalmol. Vis. Sci 54, 8270–8274. [PubMed: 24302585]

Wang Y, Chen S, Liu Y, Huang W, Li X, Zhang X, 2018 Inflammatory cytokine profiles in eyes with primary angle-closure glaucoma. Biosci. Rep 38 BSR20181411.

Wei SM, Eisenberg DP, Kohn PD, Kippenhan JS, Kolachana BS, Weinberger DR, Berman KF, 2012 Brain-derived neurotrophic factor Val(6)(6)Met polymorphism affects resting regional cerebral blood flow and functional connectivity differentially in women versus men. J. Neurosci 32, 7074–7081. [PubMed: 22593075]

Weinstein GW, Arden GB, Hitchings RA, Ryan S, Calthorpe CM, Odom JV, 1988 The pattern electroreti nogram (PERG) in ocular hypertension and glaucoma. Arch. Ophthalmol 106, 923–928. [PubMed: 3390056]

Wells-Gray EM, Choi SS, Slabaugh M, Weber P, Doble N, 2018 Inner retinal changes in primary open-angle glaucoma revealed through adaptive optics-optical coherence tomography. J. Glaucoma 27, 1025–1028. [PubMed: 30095607]

Wolff B, Basdekidou C, Vasseur V, Mauget-Faysse M, Sahel JA, Vignal C, 2013 Retinal inner nuclear layer microcystic changes in optic nerve atrophy: a novel spectral-domain OCT finding. Retina 33, 2133–2138. [PubMed: 23644558]

Wolff B, Azar G, Vasseur V, Sahel JA, Vignal C, Mauget-Faysse M, 2014 Microcystic changes in the retinal internal nuclear layer associated with optic atrophy: a prospective study. J. Ophthalmol 2014, 395189. [PubMed: 24701345]

Wollstein G, Schuman JS, Price LL, et al., 2005 Optical coherence tomography longitudinal evaluation of retinal nerve fiber layer thickness in glaucoma. Arch. Ophthalmol 123, 464–470. [PubMed: 15824218]

Wollstein G, Kagemann L, Bilonick RA, Ishikawa H, Folio LS, Gabriele ML, Ungar AK, Duker JS, Fujimoto JG, Schuman JS, 2012 Retinal nerve fibre layer and visual function loss in glaucoma: the tipping point. Br. J. Ophthalmol 96, 47–52. [PubMed: 21478200]

Wong TT, Zhou L, Li J, Tong L, Zhao SZ, Li XR, Yu SJ, Koh SK, Beuerman RW, 2011 Proteomic profiling of inflammatory signaling molecules in the tears of patients on chronic glaucoma medication. Invest. Ophthalmol. Vis. Sci 52, 7385–7391. [PubMed: 21697136]

Wong JJ, Chen TC, Shen LQ, Pasquale LR, 2012 Macular imaging for glaucoma using spectral-domain optical coherence tomography: a review. Semin. Ophthalmol 27, 160–166. [PubMed: 23163271]

Wong-Riley MT, 2010 Energy metabolism of the visual system. Eye Brain 2, 99–116. [PubMed: 23226947]

Wu Z, Medeiros FA, 2018 Recent developments in visual field testing for glaucoma. Curr. Opin. Ophthalmol 29, 141–146. [PubMed: 29256895]

Wu Z, Lin C, Crowther M, Mak H, Yu M, Leung CK, 2017 Impact of rates of change of lamina cribrosa and optic nerve head surface depths on visual field progression in glaucoma. Invest. Ophthalmol. Vis. Sci 58, 1825–1833. [PubMed: 28353690]

Xu LJ, Zhang L, Li SL, Zemon V, Virgili G, Liang YB, 2017 Accuracy of isolated-check visual evoked potential technique for diagnosing primary open-angle glaucoma. Doc. Ophthalmol 135, 107–119. [PubMed: 28702796]

Yamanari M, Miura M, Makita S, Yatagai T, Yasuno Y, 2008 Phase retardation measurement of retinal nerve fiber layer by polarization-sensitive spectral-domain optical coherence tomography and scanning laser polarimetry. J. Biomed. Optic 13, 014013.

Yang XL, van der Merwe Y, Sims J, Parra C, Ho LC, Schuman JS, Wollstein G, Lathrop KL, Chan KC, 2018 Age-related changes in eye, brain and visuomotor behavior in the DBA/2J mouse model of chronic glaucoma. Sci. Rep 8, 4643. [PubMed: 29545576]

Yap TE, Donna P, Almonte MT, Cordeiro MF, 2018a Real-time imaging of retinal ganglion cell apoptosis. Cells 7, 60.

Yap ZL, Verma S, Lee YF, Ong C, Mohla A, Perera SA, 2018b Glaucoma related retinal oximetry: a technology update. Clin. Ophthalmol 12, 79–84. [PubMed: 29379268]

Yi J, Chen SY, Shu X, Fawzi AA, Zhang HF, 2015 Human retinal imaging using visible-light optical coherence tomography guided by scanning laser ophthalmoscopy. Biomed. Optic Express 6, 3701–3713.

Zakharov P, Völker AC, Wyss MT, Haiss F, Caleinaghi N, Zunzunegui C, Buck A, Scheffold F, Weber B, 2009 Dynamic laser speckle imaging of cerebral blood flow. Optic Express 17, 13904–13917.

Zawadzki RJ, Cense B, Zhang Y, Choi SS, Miller DT, Werner JS, 2008 Ultrahigh-resolution optical coherence tomography with monochromatic and chromatic aberration correction. Optic Express 16, 8126–8143.

Zawadzki RJ, Choi SS, Fuller AR, Evans JW, Hamann B, Werner JS, 2009 Cellular resolution volumetric in vivo retinal imaging with adaptive optics-optical coherence tomography. Optic Express 17, 4084–4094.

Zeitz O, Galambos P, Wagenfeld L, Wiermann A, Wlodarsch P, Praga R, Matthiessen ET, Richard G, Klemm M, 2006 Glaucoma progression is associated with decreased blood flow velocities in the short posterior ciliary artery. Br. J. Ophthalmol 90, 1245–1248. [PubMed: 16825276]

Zemon V, Gordon J, Welch J, 1988 Asymmetries in ON and OFF visual pathways of humans revealed using contrast-evoked cortical potentials. Vis. Neurosci 1, 145–150. [PubMed: 3154786]

Zemon V, Eisner W, Gordon J, Grose-Fifer J, Tenedios F, Shoup H, 1995 Contrast-dependent responses in the human visual system: childhood through adulthood. Int. J. Neurosci 80, 181–201. [PubMed: 7775048]

Zhang X, Hu J, Knighton RW, Huang XR, Puliafito CA, Jiao S, 2011 Dual-band spectral-domain optical coherence tomography for in vivo imaging the spectral contrasts of the retinal nerve fiber layer. Optic Express 19, 19653–19659.

Zhang Y, Liang W, Wu G, Zhang X, Wen G, 2016 Magnetization transfer imaging reveals geniculocalcarine and striate area degeneration in primary glaucoma: a preliminary study. Acta Radiologica. Open 5, 2058460116666876.

Zhang T, Kho A, Srinivasan VJ, 2019a. Improving visible light OCT of the human retina with rapid spectral shaping and axial tracking. Biomed. Optic Express 10, 2918–2931.

Zhang X, Parrish RK 2nd, Greenfield DS, Francis BA, Varma R, Schuman JS, Tan O, Huang D, 2019b Predictive factors for the rate of visual field progression in the advanced imaging for glaucoma study. Am. J. Ophthalmol 202, 62–71. [PubMed: 30794787]

Zhou W, Muir ER, Chaffin S, Nagi KS, Duong TQ, 2017 MRI study of the posterior visual pathways in primary open angle glaucoma. J. Glaucoma 26, 173–181. [PubMed: 27661989]

Zotter S, Pircher M, Torzicky T, Baumann B, Yoshida H, Hirose F, Roberts P, Ritter M, Schutze C, Gotzinger E, Trasischker W, Vass C, Schmidt-Erfurth U, Hitzenberger CK, 2012 Large-field high-speed polarization sensitive spectral domain OCT and its applications in ophthalmology. Biomed. Optic Express 3, 2720–2732.

Zotter S, Pircher M, Gotzinger E, Torzicky T, Yoshida H, Hirose F, Holzer S, Kroisamer J, Vass C, Schmidt-Erfurth U, Hitzenberger CK, 2013 Measuring retinal nerve fiber layer birefringence, retardation, and thickness using wide-field, high-speed polarization sensitive spectral domain OCT. Invest. Ophthalmol. Vis. Sci 54, 72–84. [PubMed: 23221076]
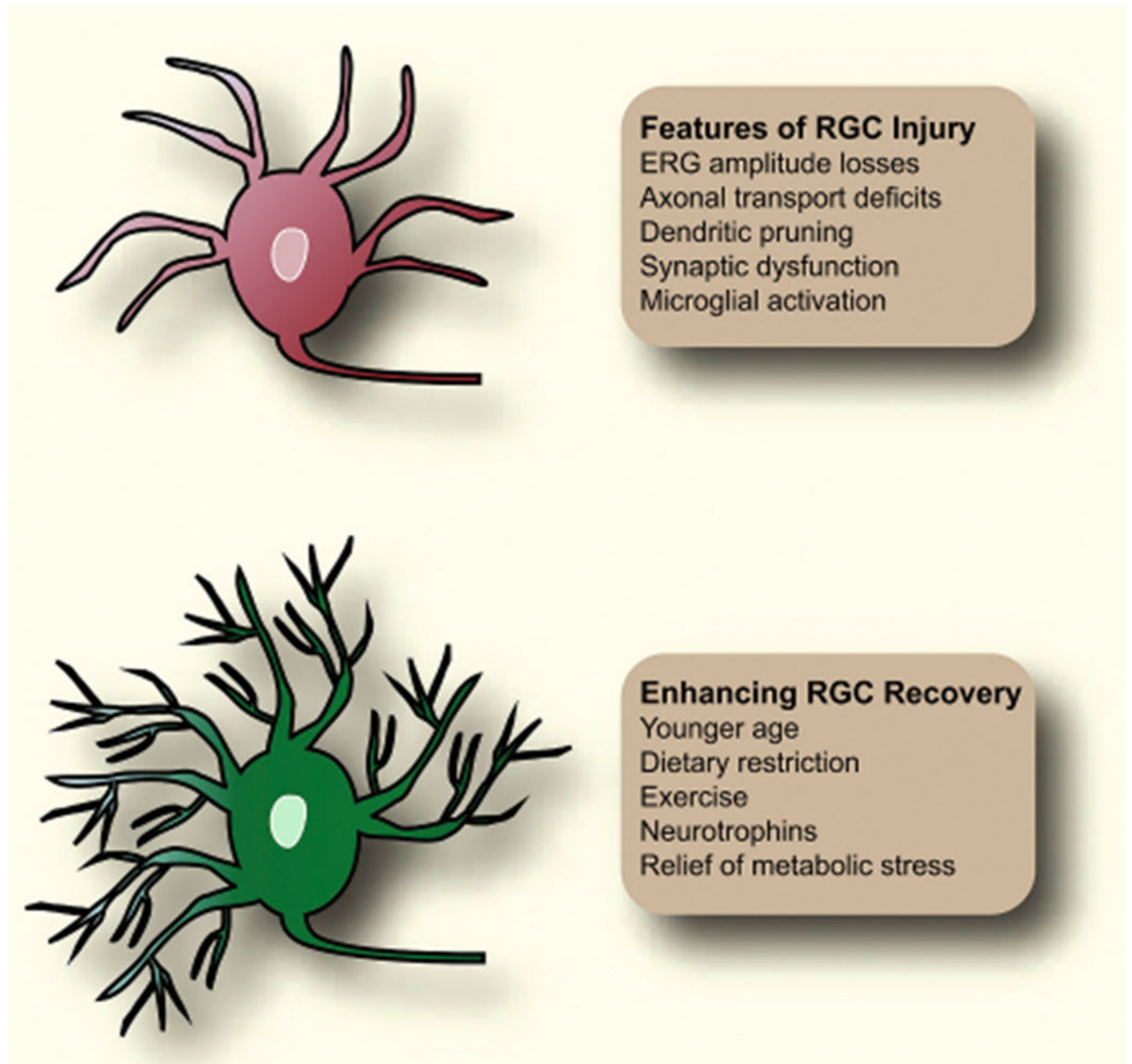
Fig. 1.
Schematic model of RGC injury and recovery. RGCs may enter a 'comatose' state, where functional impairment occurs following cellular insults in glaucoma. Relief of RGC stress may allow for RGC functional recovery, however injuries of a sufficient magnitude, duration or quantity may trigger irreversible cell death. Figure and legend reproduced with permission from Elsevier (Fry et al., 2018).
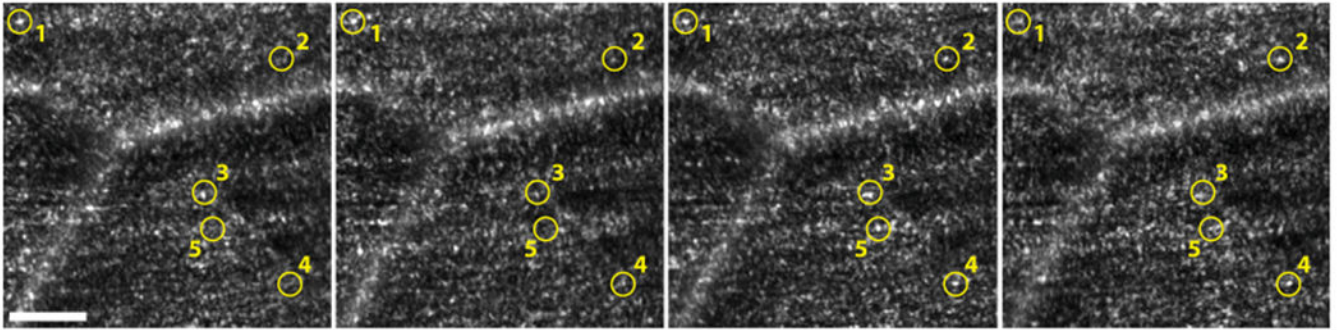
Fig. 2.
Punctate backscattering/reflectivity changes in the innermost surface of the RNFL in a healthy control as seen in confocal reflectance adaptive optics ophthalmoscopy images captured a few seconds apart. Scale bar, 50 μm.
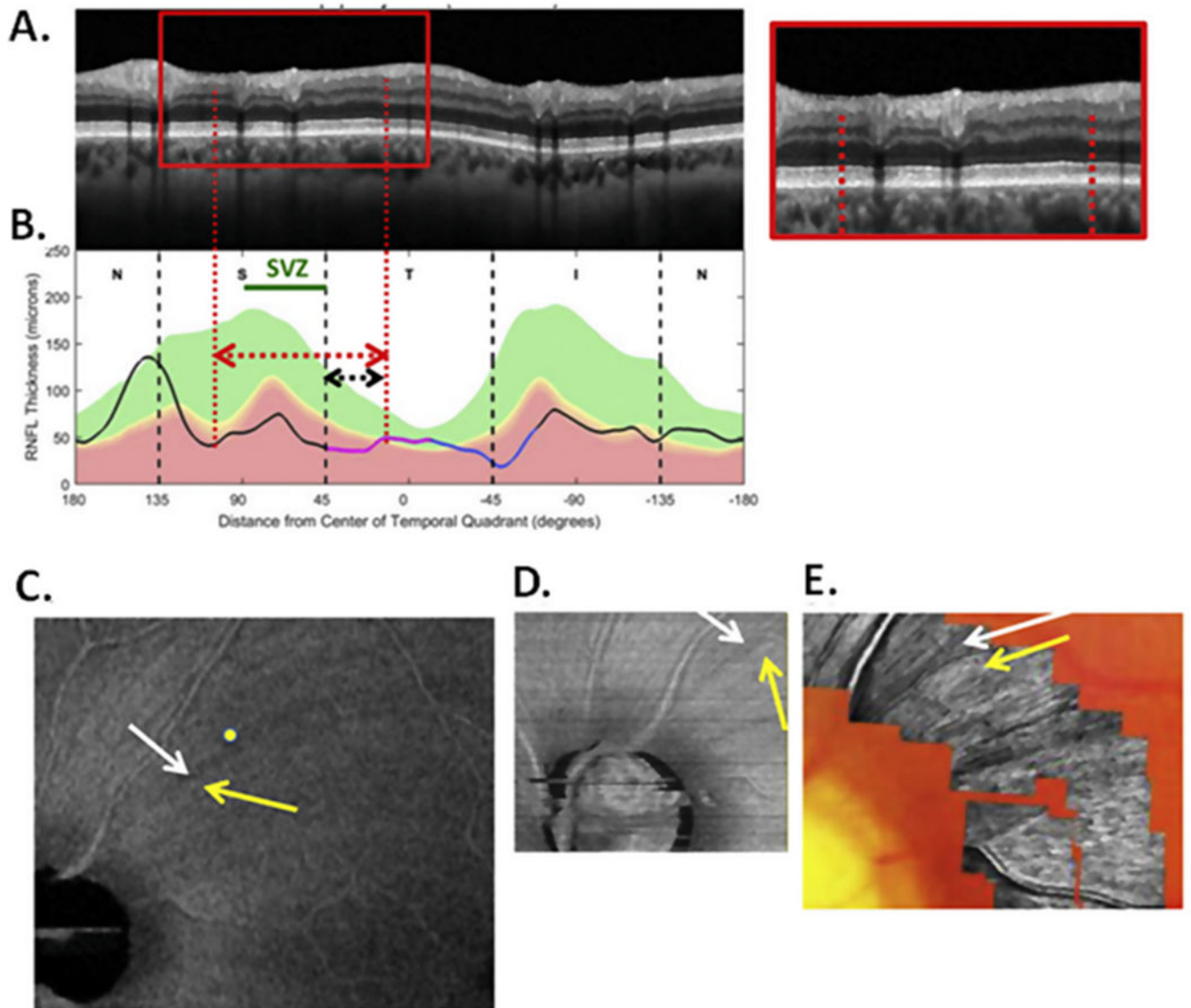
Fig. 3.
The sdOCT results for an eye with widespread cpRNFL damage. (A) An image from a circumpapillary scan. (B) The cpRNFL thickness plot (black, magenta, and light blue curve). The SVZ is shown as the green line. (C) An en-face slab image of the 9 * 12 mm scan. (D) An en-face slab image of a 3 * 3 mm scan of disc. (E) AO-SLO image. The yellow and white arrows are approximately the same locations in panels (C), (D), and (E). Figure and legend reproduced with permission and modified from Elsevier (Hood et al., 2017).

Anatomical MRI of Optic Nerve and Optic Chiasm
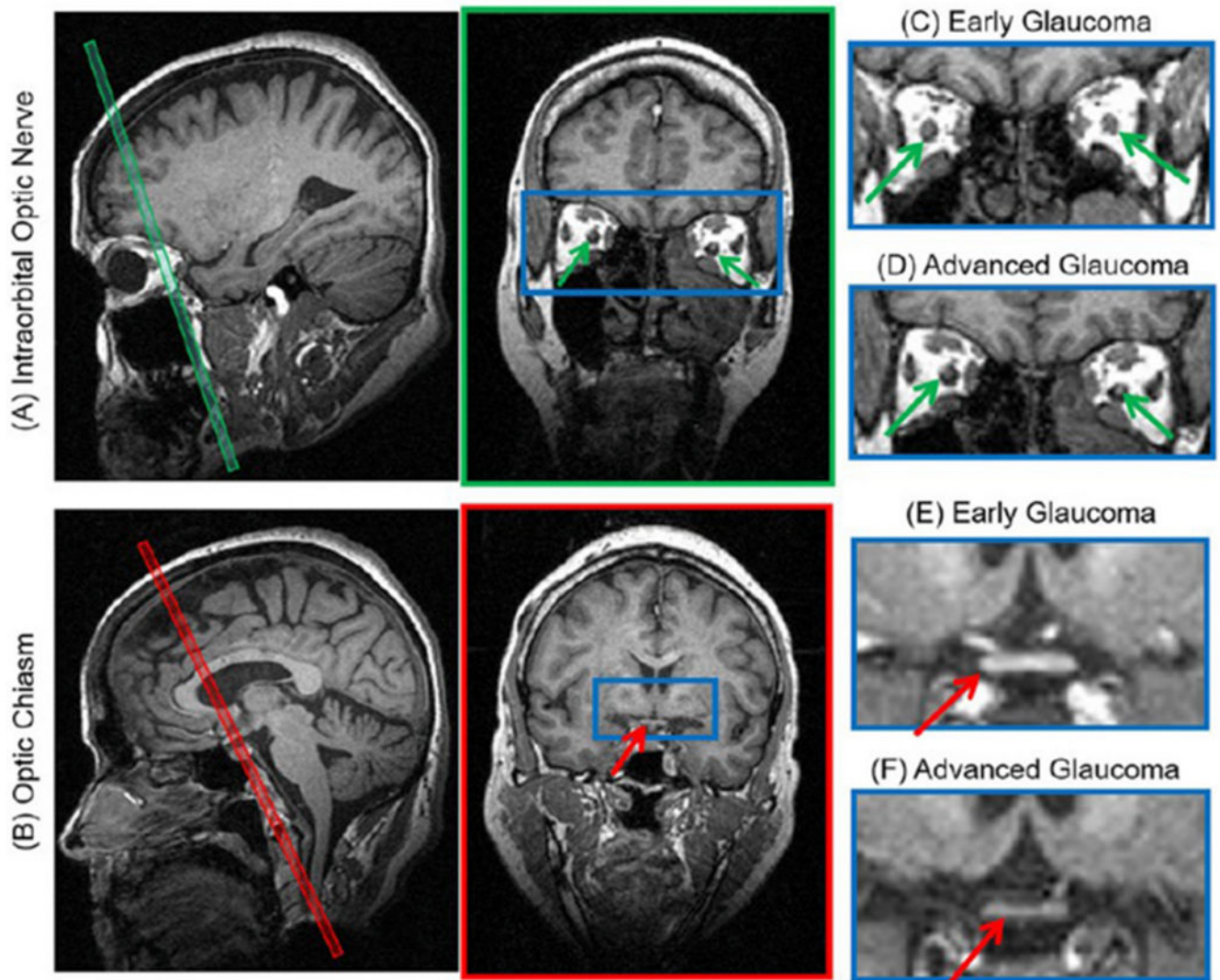
Fig. 4.
Structural brain MRI in early and advanced glaucoma. (A, B) Anatomical MRI of the intraorbital optic nerve (A) and optic chiasm (B) in sagittal view (left) and coronal view (right) at the level of the green or red slab. (C–F) Zoomed images of the intraorbital optic nerve (green arrows) (C, D) and optic chiasm (red arrows) (E, F) from the blue boxes in A, B in early E) and advanced glaucoma (D, F). Note the reduction in size in both structures as the disease progresses. Figure and legend reproduced with permission and modified from Wolters Kluwer - Medknow Publications (Kasi et al., 2019).
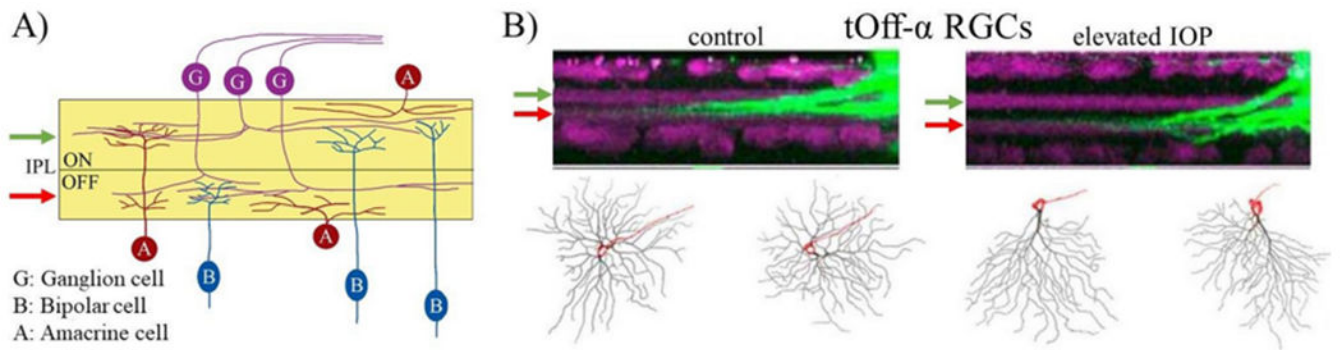
Fig. 5.
(A) RGC-type specific lamination patterns in the ON- and OFF- sublaminae. (B) Dendritic rearrangements of OFF-transient RGCs have been implicated as among the earliest responses to elevated IOP in mice. Figure and legend reproduced with permission and modified from Society for Neuroscience (El-Danaf and Huberman, 2015).
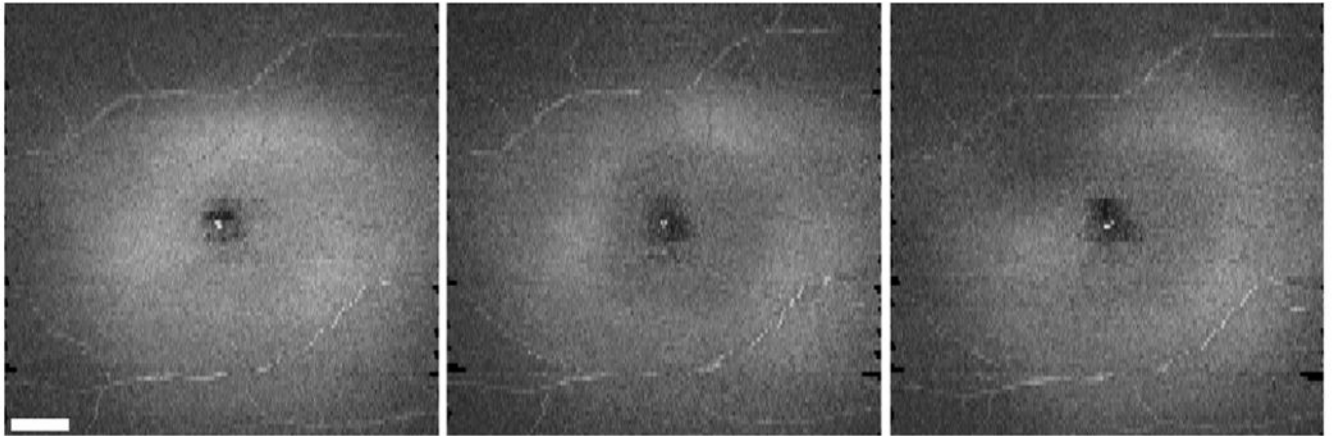
Fig. 6.
IPL reflectivity maps captured using near infrared OCT in a normal control, a few minutes apart. The changes in intensity near the foveal pit and the top left quadrant suggest that poor repeatability might limit the potential for using IPL intensity in OCT images as a glaucoma biomarker. Scale bar, 1 mm.
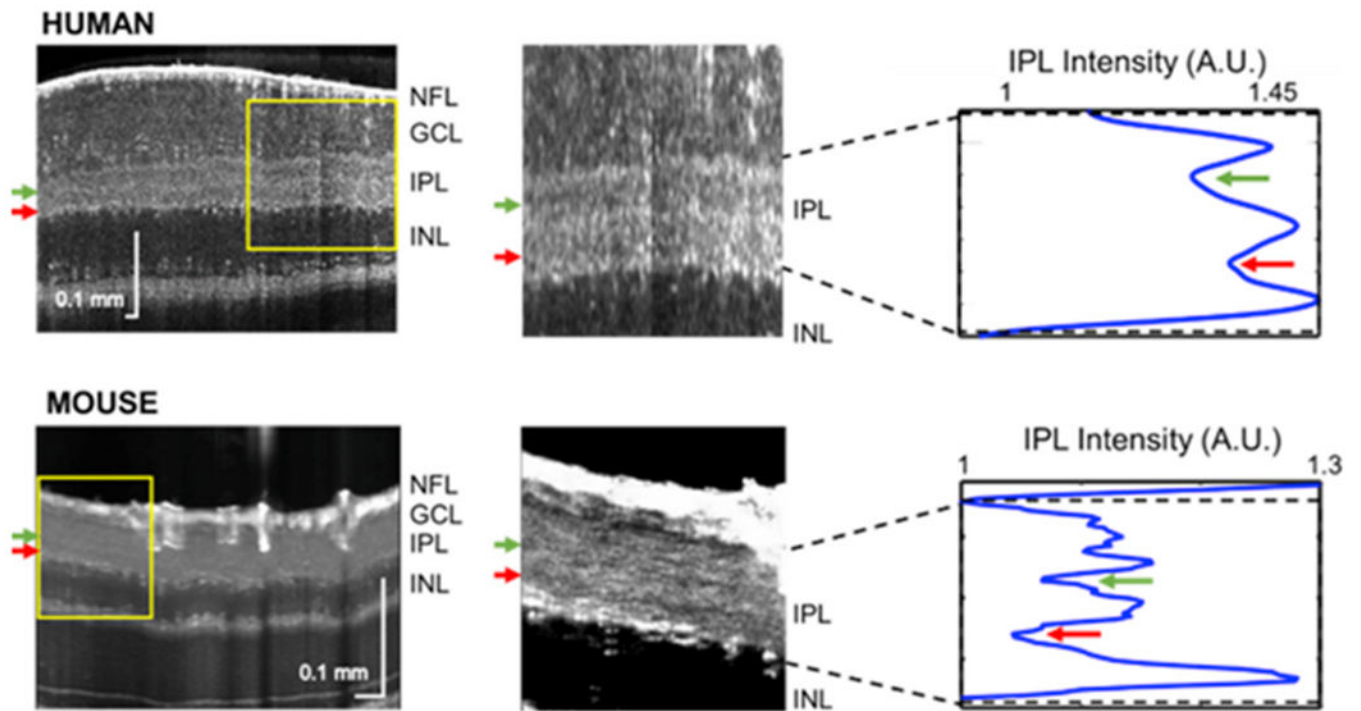
Fig. 7.
Visible light OCT cross-sectional images reveal a reflectivity pattern corresponding to inner plexiform layer (IPL) lamination in humans (A) and mice (B). Cell-type specific lamination patterns previously described for ON- and OFF-RGC sublaminae correspond well with the reflectivity pattern (C).
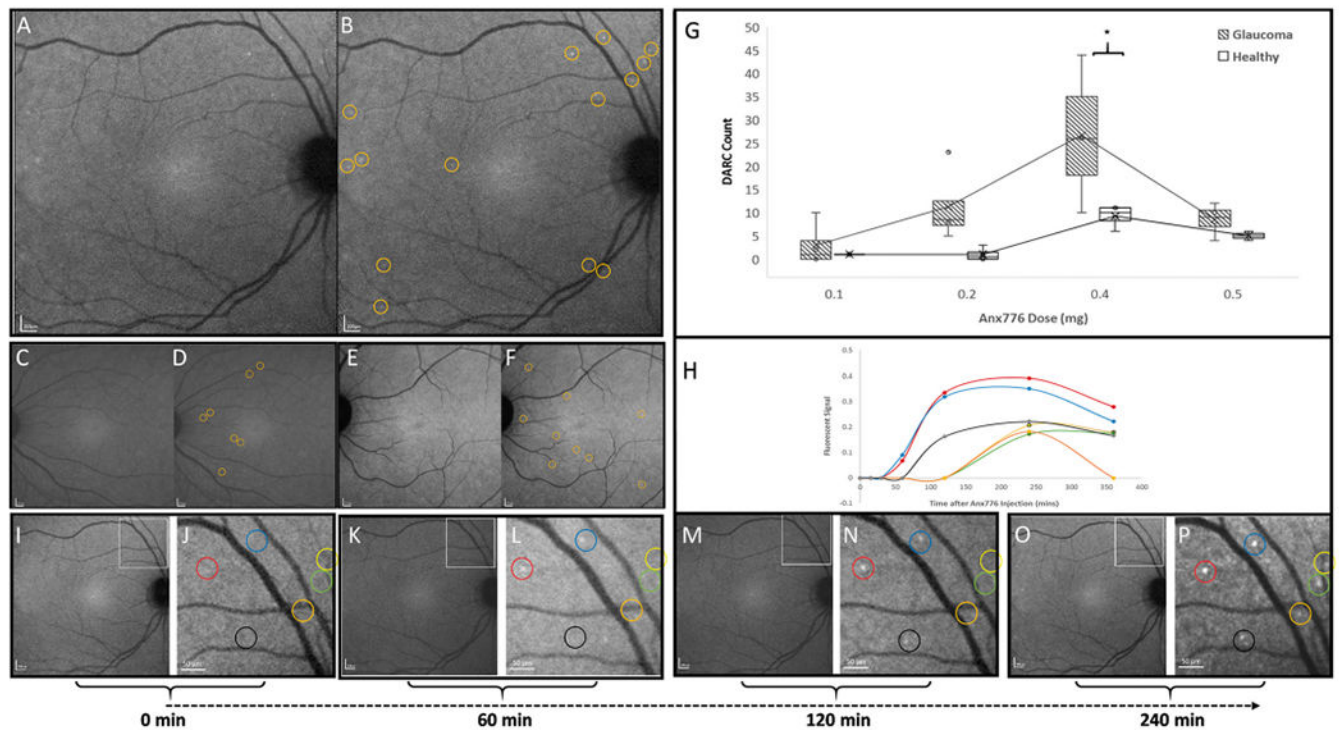
Fig. 8.
DARC counts are increased in affected glaucoma patients compared to healthy controls. ANX776 injections revealed single neuronal cell apoptosis in the retina of study subjects. Representative retinal images are shown from glaucoma patients following intravenous injections of 0.4 (A and B), 0.2 (C and D) and 0.5 (E and F) mg ANX776 at 240 min. Panels show unmarked (A, C and E) and marked (B, D and F) ANX776-positive spots with yellow rings highlighting individual spots. DARC counts were defined as new, unique individual ANX776-labeled spots, at their first appearance in the retina. Analysis of DARC counts in glaucoma and healthy controls for each ANX776 dosing cohort showed that at each dose, the number of DARC spot counts was consistently higher in glaucoma patients compared to healthy controls, and this reached significance at the 0.4 mg (P < 0.005) dose (G). The spread of the individual data points is shown in Tukey's box plots (G). Horizontal lines indicate medians and interquartile ranges with the continuous line across doses showing the means. Asterisks indicate the level of significance by Bonferroni multiple comparison test between groups (P < 0.01) with two-way ANOVA across the doses showing a significant effect of glaucoma status (P = 0.0033) and time point (P = 0.0011). Multivariable analysis indicated that the total DARC count across 6 h was 2.37-fold higher in patients with glaucoma (95% CI: 1.4–4.03, P = 0.003) at any dose. Different fluorescent intensity profiles were seen for individual labeled spots (H–P). Low (I, K, M and O) and high (J, L, N and P) magnification (scale bars indicated) retinal images at different time points are shown from the same patient as in A at baseline (I and J, 0 min), 60 (K and L), 120 (M and N) and 240 (O and P) min. Marked, colour-coded spots are shown in adjacent panels (J, L, N and P) with fluorescent intensity profiles illustrated in H, identified by corresponding coloured

lines. Figure and legend reproduced with permission from Oxford University Press (Cordeiro et al., 2017).
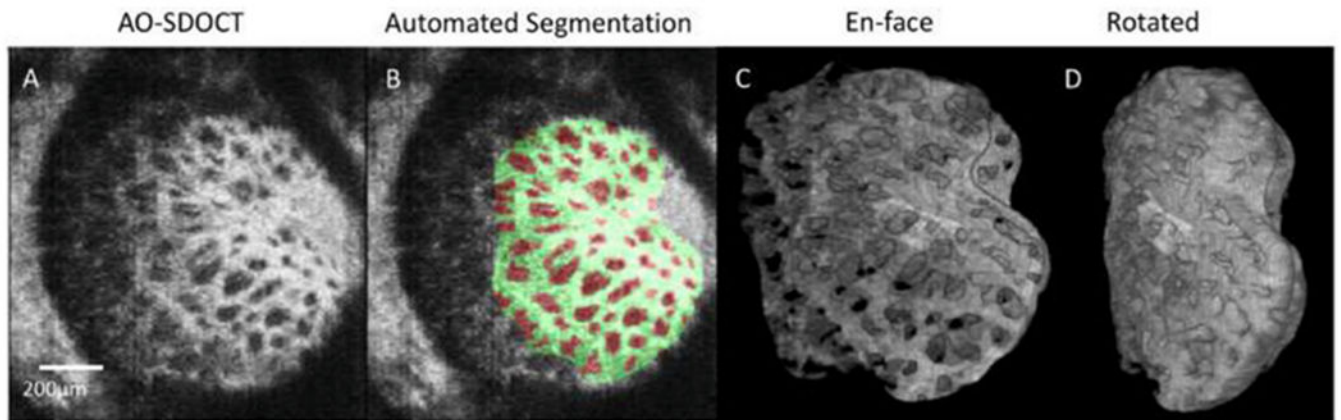
Fig. 9.
(A) Original C-mode of adaptive optics OCT taken from a 56-year-old Caucasian woman with glaucoma. (B) Automated segmentation of the corresponding slice, with the beams labeled in green and pores in red. (C) 3D view en-face of the LC beams. (D) rotated 3D view of the same LC beams. Figure and legend reproduced with permission from Elsevier (Dong et al., 2017).
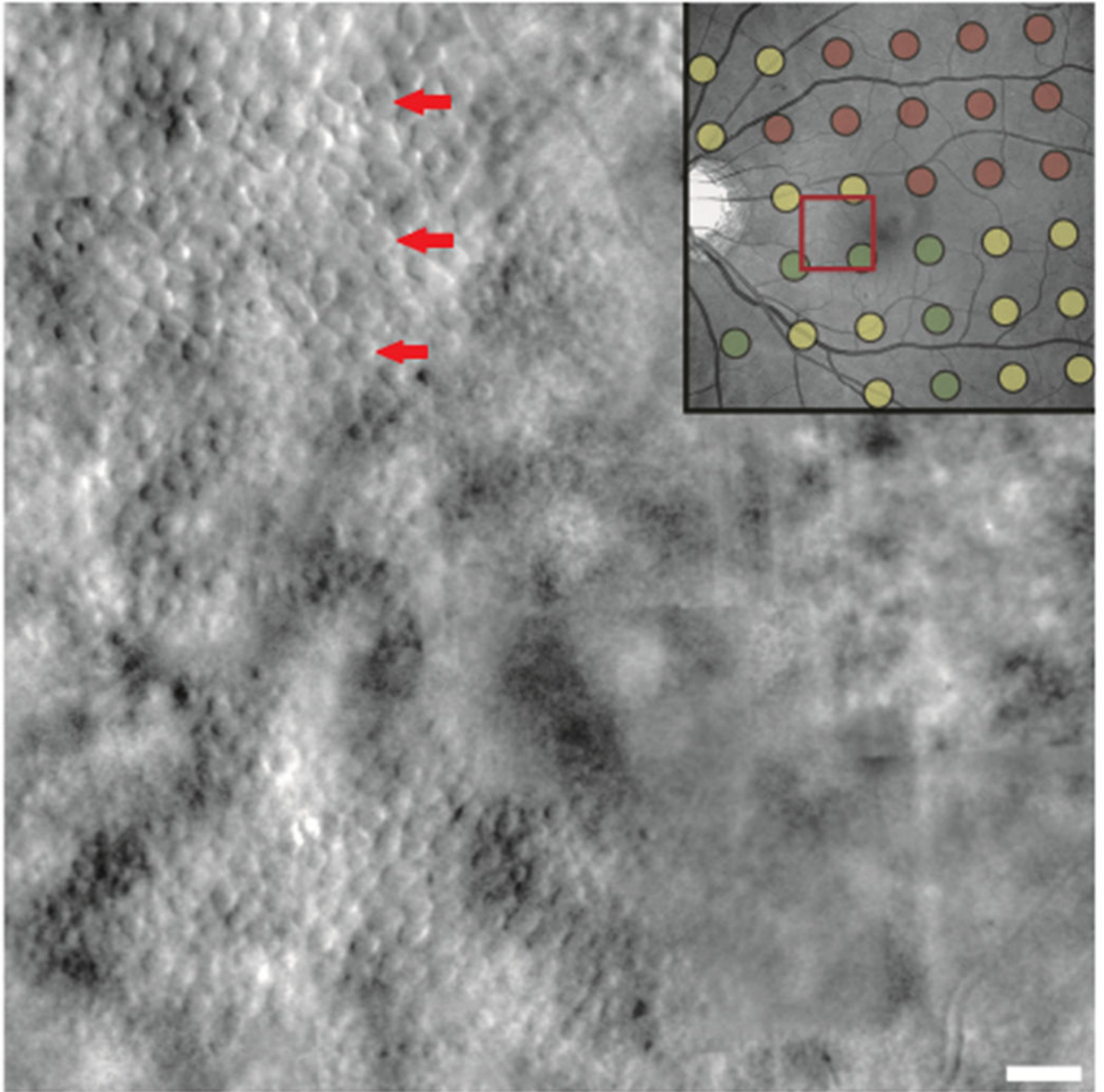
Fig. 10.
Densely packed macular INL micro cystoid spaces (red arrows) in a primary open-angle
glaucoma patient as seen with non-confocal split-detection AO ophthalmoscopy. The scale
bar is 100 μm across. This retinal area, highlighted as a red square in the wider field of view
image (top right), shows early signs of vision loss as illustrated by the superimposed visual
field test results. The stimulus locations and size are shown by the black circles (24-2 visual
field test points, Goldmann III), with the color denoting deviation from normal on the total
deviation map (green   4 points, yellow 4–12 points and red   12 points).

Fig. 11.
Sparse INL micro cystoid spaces in a primary open-angle glaucoma patient as seen with non-confocal split-detection adaptive optics ophthalmoscopy, with its location highlighted in red in the wider field of view image (bottom left). The scale bar is 100 μm across. These micro cystoid spaces have irregular shapes and sizes as large as 40 μm, which is substantially larger than the bodies of cells in this layer (see legend box).
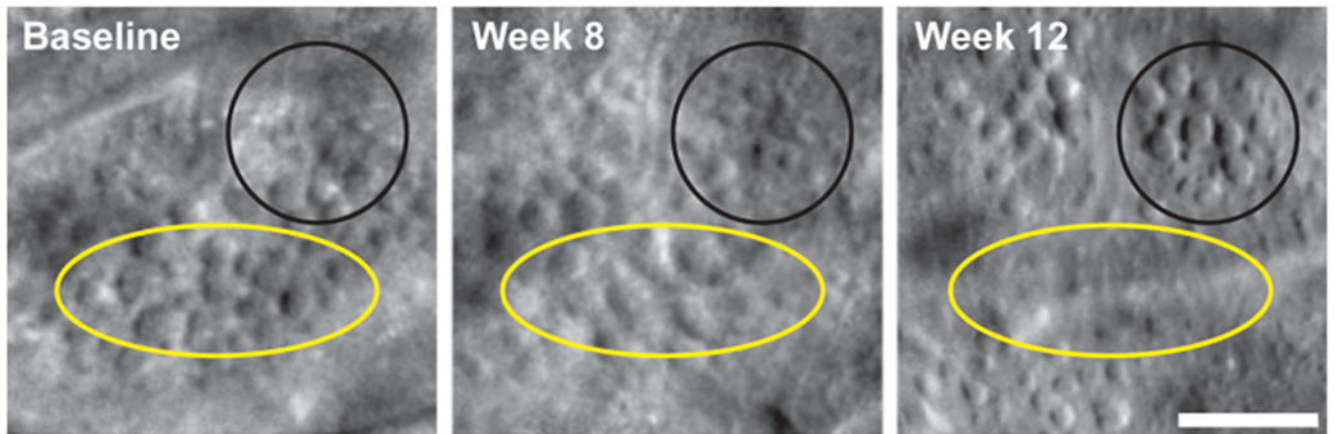
Fig. 12.
INL microcystoid spaces progression (black circle) and regression (yellow ellipse) in a glaucoma patient over a four-week period, as seen with non-confocal split-detection adaptive optics ophthalmoscopy. Scale bar, 100 μm.
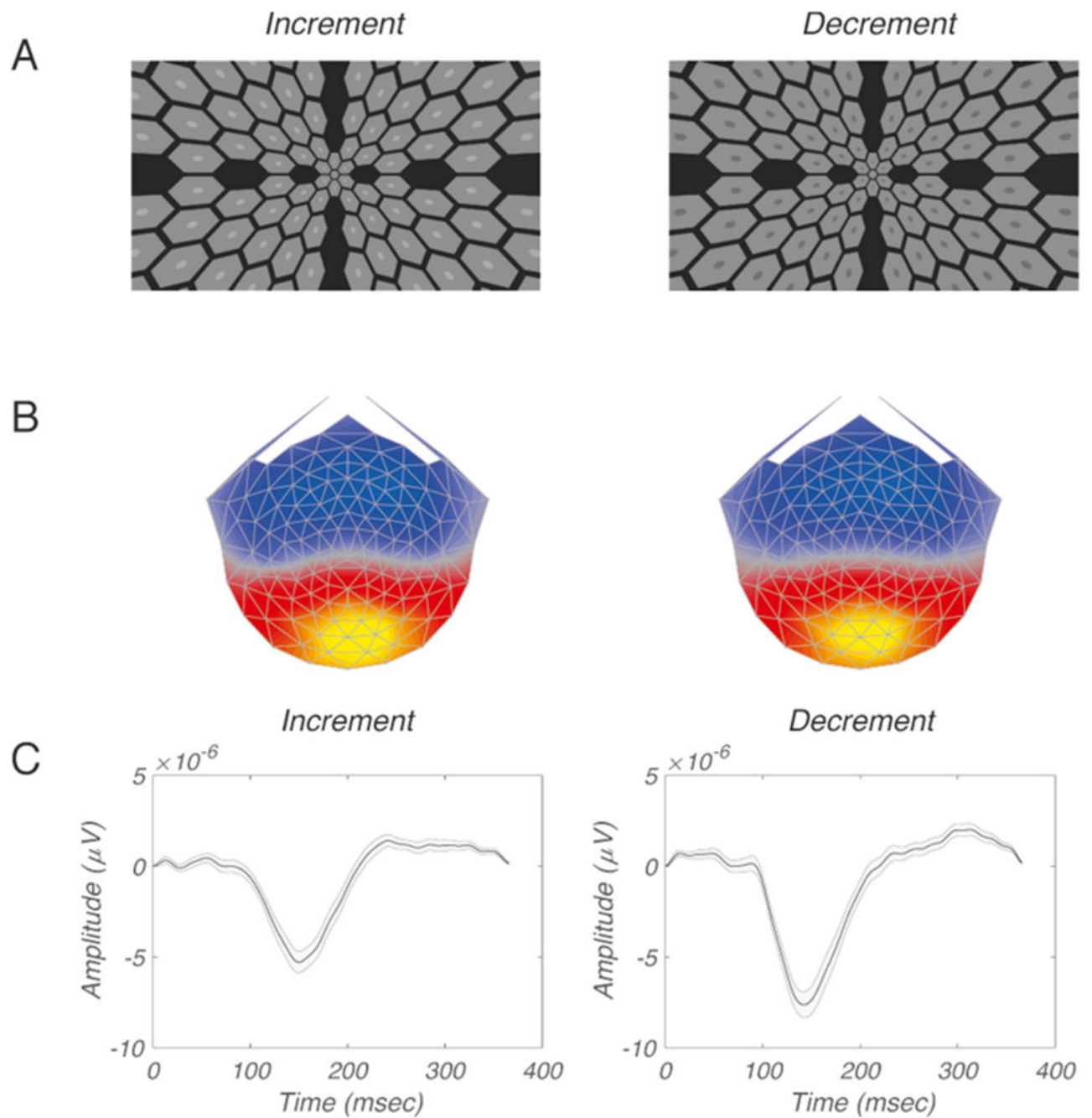
Fig. 13.

(A) Schematic illustration of stimulus array used to measure increment responses (left panel) and decrement responses (right panel). Array elements are scaled to account for cortical magnification. (B) Scalp topography of the most reliable response component is similar for increments (left panel) and decrements (right panel). Components measured using Reliable Components Analysis (Dmochowski et al., 2015). (C) Waveform of the most reliable

component evoked by 2.7 Hz incremental (left) or decremental (right) sawtooth waveforms. Response to decrements is larger than for increments (n = 14; healthy 18–22 age observers).